FORMATE METABOLISM IN THE RAT

GREGORY P. MORROW

Formate Metabolism in the Rat

by

© Gregory P. Morrow

A Thesis submitted to the

School of Graduate Studies

in partial fulfillment of the requirements for the degree of

Master of Science

Department of Biochemistry, Faculty of Science

Memorial University of Newfoundland

August, 2012

St. John's   Newfoundland

Abstract

The folate-associated one-carbon (1C) metabolic pathways provide the building blocks for key components of DNA (thymidylate and purines), as well as the supply of methyl groups for methyltransferases. The free formate pool plays an essential role in the transport of one-carbon units from production to utilization. An enzymatic assay was optimized for the determination of the plasma formate concentration in rats under normal and folate-deficient conditions. Stable isotope tracer infusions were used to quantify the endogenous production rates of formate; this amounted to 75 μmol/hr/100 g body weight in folate-replete rats, dropping to 45 μmol/hr/100 g body weight in folate-deficient rats. This means that, in (healthy) folate-replete rats, endogenous formate production accounts for ∼35% of the total ingested potential 1C groups (44% of that remaining after accounting for net protein synthesis). This could indicate that formate production is a central component of the metabolism of some of these 1C precursors. We investigated the importance of known dietary 1C precursors to the 1C pool through a dietary precursor supplementation study. Serine, histidine, and choline were found to be significant precursors to formate.

Acknowledgements

Table of Contents

List of Tables

List of Figures

List of Abbreviations

1C	One-carbon
AIN	American Institute of Nutrition
AMT	Aminomethyltransferase
amu	atomic mass unit
BHMT	Betaine:homocysteine methyltransferase
DMG	Dimethylglycine
DTT	Dithiothreitol
FDH	Formate Dehydrogenase
FIGLU	Formiminoglutamate
GC-MS	gas chromatograph with mass spectrometer
GCS	Glycine cleavage system
GNMT	Glycine-N-methyltrasnferase
HPLC	High Performance Liquid Chromatograph
INT	Iodonitrotetrazolium
MTHFR	5,10-methylene tetrahydrofolate reductase
NMR	Nuclear magnetic resonance
PFBBr	Pentafluorobenzyl bromide
PMS	Methoxy 5-methyl phenazinium methylsulfate
SAH	S-adenosyl homocysteine
SAM	S-adenosyl methionine
SGR	Specific growth rate
SHMT	Serine-hydroxymethyltransferase

THF   Tetrahydrofolate

TTR   Tracer: tracee ratio

USP   United States Pharmacopeia

WST-1   Water soluble tetrazolium-1 salt

List of Appendices
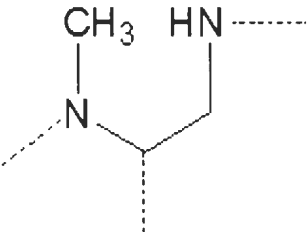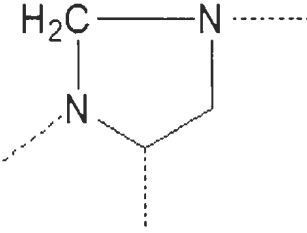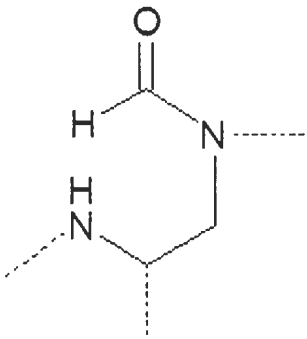
Chapter One - Introduction

1.1 One-carbon metabolism

One-carbon metabolism refers to the set of reactions which procure single carbon units, primarily from dietary sources, for the production of DNA bases (purines and thymidylate) as well as providing methyl units for S-adenosyl methionine (SAM, the universal methyl donor)(*1*). This pool of one-carbon units is created and replenished by the catabolism of a variety of precursors (primarily amino acids and choline) found in the diet (*2*). Some of these reactions provide a single one-carbon unit, while others are capable of donating several one-carbon units through consecutive catabolic reactions. Many of these reactions require a folate co-substrate for the reaction to proceed, whereas others proceed independently. In the case of those pathways requiring folate as a co-substrate, the resultant one-carbon unit will be integrated into a folate structure. In the absence of a folate, the one-carbon group produced will be formate, the simplest carboxylic acid.

Prior to utilization, one-carbon groups must be integrated into the folate pool. They can then be shuttled to their respective usages. In this manner, a cell's complete one-carbon pool exists as both free formate as well as one-carbon groups, in a variety of oxidation states, associated with tetrahydrofolate (THF) (see Table 1.1). The body has several ways of eliminating excess one-carbon groups, including oxidation to carbon dioxide or through the excretion of formate in the urine. Figure 1.1 provides a simplified schema for one-carbon metabolism in the context of a hepatic cell.

Table 1.1 Oxidation states, and corresponding structures, of common folate-bound one-carbon groups and the associated free molecules below.

Folate-bound one-carbon	Structure	Equivalent Free Molecule
5-methyl THF		Methanol CH_3OH
5,10-methylene THF		Formaldehyde HCHO
10-formyl THF		Formic Acid HCOOH

Note: This table is an abridged version of a similar table found on page 114 of the above citation (2). This is included due to the importance of these structures to the work contained in this thesis.
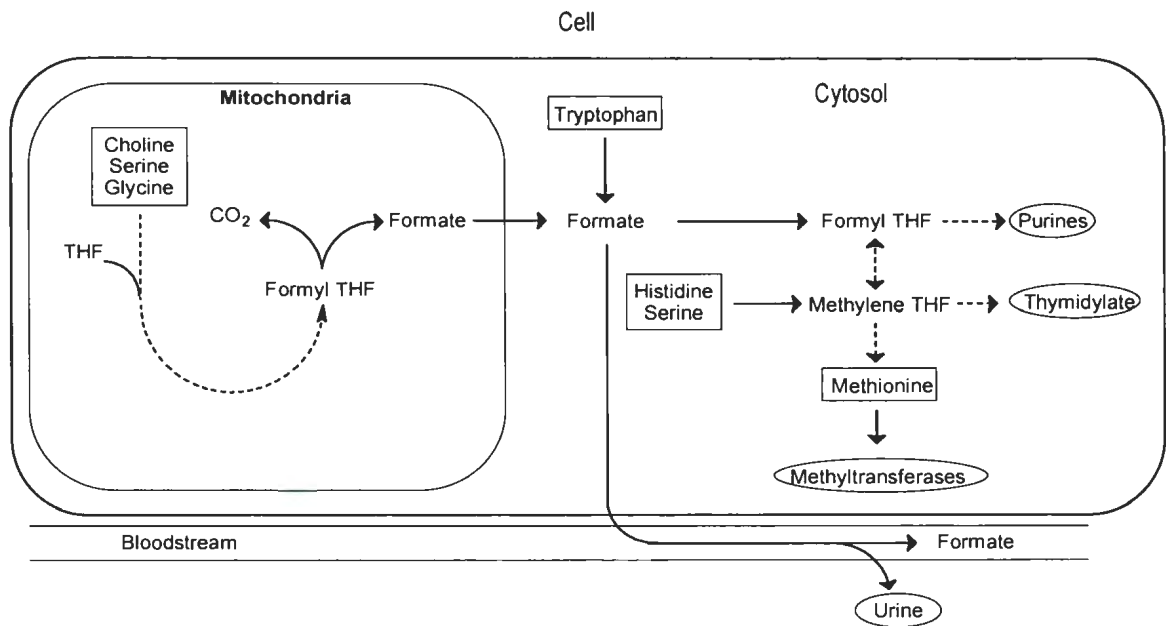
Figure 1.1. A simplified representation of the flow of one-carbon groups within a hepatic cell. One-carbon precursors are surrounded by a box. Reactions/processes consuming or removing one-carbon units from the cellular pool are highlighted with an oval. Bound one-carbon groups (indicated with a THF) are restricted to either the cytoplasm or mitochondria, whereas free formate can be transported across the mitochondrial membrane.

4

1.2 Folate

Folate, in the broadest definition, can be considered as a water-soluble B-vitamin (B9), derived either naturally from the diet (primarily dark green leafy vegetables such as spinach) or synthetically as a more oxidized product, folic acid (3). Despite some structural differences between these two sources, the backbone of both forms of this vitamin is identical (see Figure 1.2). The one-carbon binding domain is located on a pteridine structure, with one-carbon groups binding to one or both of the N5 or N10 atoms(4). The pteridine structure is bound to a p-aminobenzoic acid derivative, which in turn connects to a glutamate tail of between one and eight residues connected by isopeptide bonds.

A major difference between natural folate and synthetic folic acid lies in the poly-glutamate tail found in the naturally occurring variants of folate(5). Natural folate will bear a polyglutamate tail of between four and seven glutamate residues (4). Bioavailability is defined as the proportion of an ingested compound that is actually absorbed from the diet (and used by the body) to the total dietary availability (6). In the case of folate, bioavailability depends on the length of the glutamate tail. The human genome codes for a protein in the intestinal lining called glutamate carboxypeptidase II (GCPII) which cleaves polyglutamate residues, reducing the folate to a monoglutamate form. After ingestion, all residues in excess of a single glutamate must be cleaved enzymatically prior to absorption in the gut, a step which can prove rate-limiting (7). Accordingly, the absence of an extended glutamate tail on synthetically-derived folic acid can increase vitamin absorption in

5
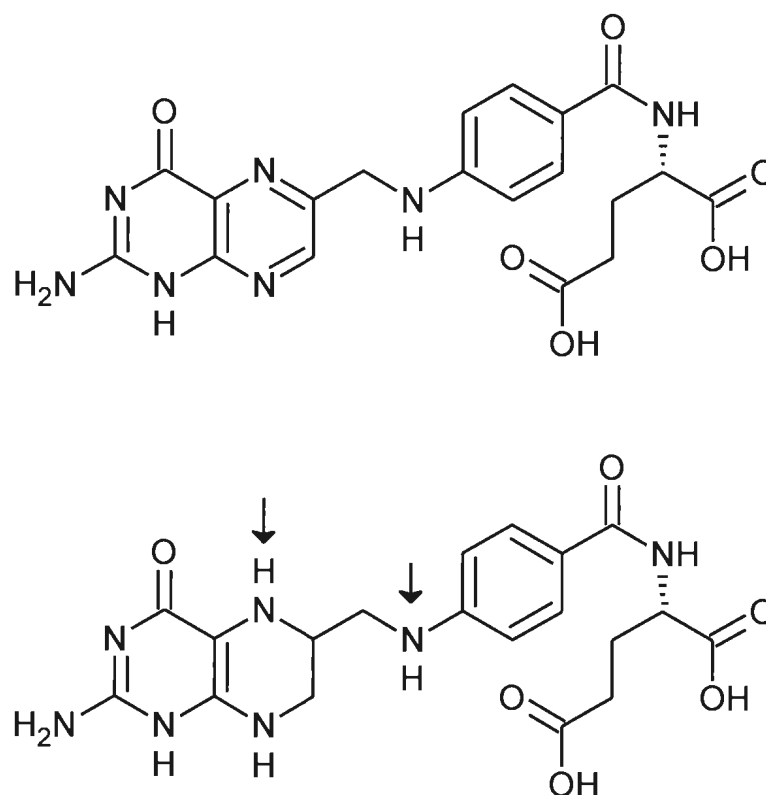
Figure 1.2. The structures of folic acid (above) and naturally occurring tetrahydrofolate (below), in the mono-glutamate form. Note the reduced double bonds on the pteridine subunit on the tetrahydrofolate structure. Arrows indicate the N5 (left) and N10 (right) positions, to which one-carbons units can be bound.

an organism. Consequently, the bioavailability of a polyglutamated folate is less than that of the monoglutamated form by 20-40%; therefore synthetic folic acid is more bioavailable than natural folate. The location and existence of this peptidase suggests a preference for absorption of monoglutamated folate.

Due to the enzymatic hydrolysis of these glutamates, all natural folates entering the cell will bear mono-glutamate tails. The final step prior to integration into one of the cellular folate pools is the introduction of a poly-glutamate tail(8). Although monoglutamate folates can be transported throughout the body, the action of folyl-polyglutamate synthetase is required to retain folates within their cellular pools. After the addition of extra glutamate residues, a folate will be able to participate in the one-carbon reactions relevant to its pool. Although one-carbon precursors and formate may travel between compartments, activated folates remain segregated. The majority of folates will be localized to either the cytoplasm or mitochondria with a smaller portion in the nucleus (4).

The second difference between the dietary sources of folate is the oxidative state at which the molecule enters the body. Whereas natural folate can be integrated directly into the cellular folate pools, synthetic folic acid is produced in a more oxidized form, and must first undergo an intracellular two-step enzymatic reduction catalyzed by dihydrofolate reductase(9). This cytoplasmic reaction reduces two carbon-nitrogen double bonds located on the pteridine sub-structure to single bonds, and is necessary before synthetic folic acid can be integrated into one-carbon metabolism.

1.3 Formate increases during folate deficiency

Formic acid is the simplest carboxylic acid. Tissues responsible for formate production have not been definitively identified. It is possible some format is produced by gut microorganisms. With a pKa of ~3.7, most formic acid occurs in the body as formate (the un-protonated form) (*10*). Since incorporation of formate into the folate pool occurs in the cytoplasm and much, if not most, formate production occurs in mitochondria, a means of transporting formate from mitochondria to cytoplasm is required (*2*). Recent work from our lab has demonstrated that in addition to the elevated excretion of formate in urine during folate deficiency (*11*), the plasma formate concentration also increases up to seven-fold (*12*), compared to that in healthy folate-replete rats. Plasma formate levels under various physiological conditions are provided in Appendix A. Renal handling of formate has not been studied in detail.

In humans (but not in rats), formate is the first product in the methanol catabolism pathway. Both ocular damagae and acidosis can be attributed to the accumulation of formic acid due to methanol overdose(*12*).

1.4 Folate-mediated one-carbon production

1.4.1 Serine

The catabolism of dietary serine has the potential to yield two one-carbon groups. Serine and THF can be converted, via serine hydroxymethyltransferase (SHMT), to 5,10-methylene THF and glycine (Figure 1.3). Two separate isoforms of this enzyme are coded for in the nuclear DNA, one of which is expressed in the cytoplasm (SHMT1) and one of which is expressed in the mitochondria (SHMT2)
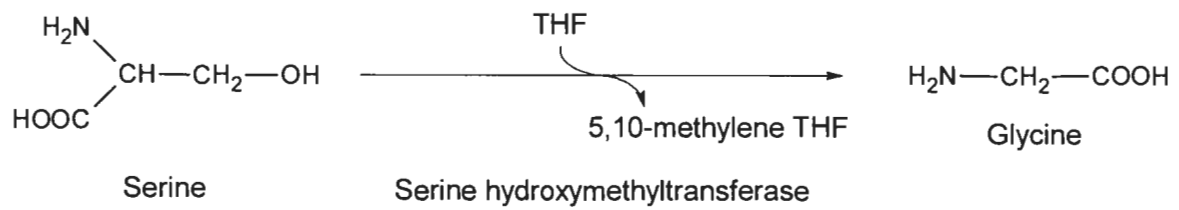
Figure 1.3. Serine hydroxymethyltransferase, using serine and THF as substrates,
produces a bound one-carbon in the form of 5,10-methylene THF as well as glycine.
The resultant glycine can either be catabolized to produce another one-carbon, or
can be used by the body for protein synthesis or other purposes.

(*13, 14*). Gregory et al. (*15*) recently employed tracer methodology to suggest that serine catabolism is responsible for the majority of one-carbon units provided for the cytoplasmic transmethylation cycle.

Stover et al. (*16*) recently used a mouse knockout model of cytoplasmic SHMT to investigate the extent of this enzyme's role in thymidylate synthesis. They found knocking out SHMT1 resulted in diminished thymidylate production along with the onset of neural tube defects in developing mouse embryos. This demonstrated the importance of serine-derived one-carbon groups in thymidylate biosynthesis. Further work by Anderson and Stover (*17*) demonstrated that the mitochondrial SHMT2 gene has an alternate splice variant that allows for localization, in lesser quantities, to the cytoplasm and nucleus. Survival of mice with a homozygous SHMT1 knockout is attributed to the small activity provided by the cytoplasmic and nuclear variants of this alternate SHMT2 expression.

1.4.2 Glycine
Unlike SHMT, which is active in both the cytoplasm and mitochondria, the multi-enzyme complex responsible for the catabolism of glycine is only expressed in the mitochondria(*18*). The Glycine Cleavage System (GCS) is made up of four components acting in concert; glycine dehydrogenase, aminomethyltransferase (AMT), GCS protein H and dihydrolipoamide dehydrogenase. The GCS is also involved in the last of several sequential mitochondrial catabolic reactions that remove and activate one-carbon groups for choline (see final reaction of choline catabolic pathway, Figure 1.6).

Narisawa et al. (*18*) used a knockout mouse model in which AMT was eliminated, resulting in neural tube defects in developing mouse embryos. This highlights the importance of glycine-derived one-carbon groups produced in the mitochondria to the one-carbon pool.

1.4.3 Methionine

Methionine contributes to the cytoplasmic one-carbon pool indirectly through its incorporation into S-adenosyl methionine (SAM), which is the key substrate for the process of transmethylation (*19*) (Figure 1.4). Methyltransferases act on nucleophilic substrates, to produce methylated products and SAH (S-adenosyl-L-homocysteine). *Glycine-N-methyltransferase* (GNMT) serves in an overflow mechanism such that if the cell generates more SAM than it requires for methylation and other reactions, the methyl group may be transferred to glycine, creating sarcosine (*20*). Sarcosine is subsequently catabolized through the choline degradation pathway, thereby contributing directly to the mitochondrial 5,10-methylene THF pool. The SAH produced by methyltransferase reactions is hydrolyzed to adenosine and homocysteine. Re-methylation of homocysteine regenerates methionine with methyl groups provided by betaine (catalyzed by *betaine:homocysteine methyltransferase*) or 5-methyl THF (catalyzed by *methionine synthase*). This regeneration process requires a one-carbon unit, ultimately contributed by choline via betaine (BHMT) (*15*), serine (via cytoplasmic SHMT) (*21*), or formate.
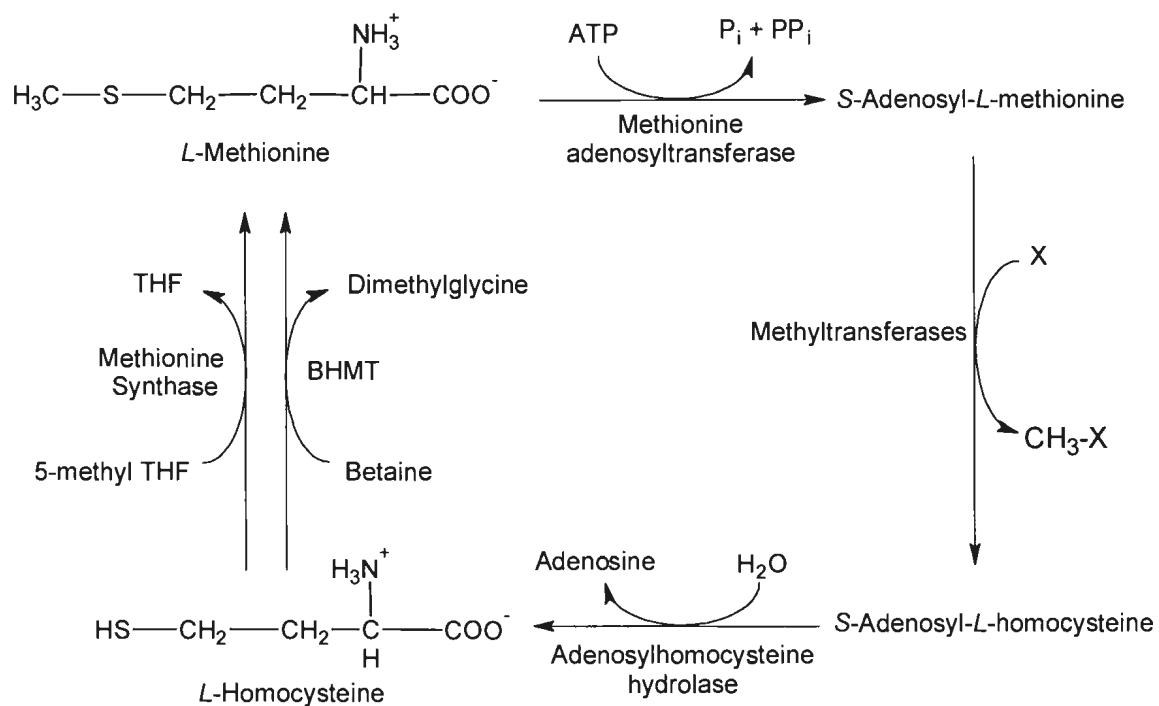
Figure 1.4. The methionine cycle in the context of one-carbon metabolism, consisting of transmethylation (SAM/SAH) and remethylation reactions (regenerating methionine from homocysteine). (BHMT: Betaine:homocysteine methyltransferase)

1.4.4 Histidine

Histidine is metabolized by a series of cytoplasmic enzymatic reactions ultimately yielding formiminoglutamate (FIGLU), as shown in Figure 1.5 (*22*). The formimino component of FIGLU is transferred to a THF co-substrate by *glutamate formiminotransferase* yielding 5-formimino THF. This is subsequently converted to 5,10-methenyl THF by 5-formimino THF cyclodeaminase. The resultant one-carbon group can then be shuttled to pathways requiring one-carbon units.

1.4.5 Choline

Choline is unique among the one-carbon precursors in that it has the ability to donate up to four of its constituent carbons to the one-carbon pool (see Figure 1.6). Choline is initially catabolized to betaine aldehyde and subsequently to betaine by choline dehydrogenase and betaine aldehyde dehydrogenase respectively (*23*). Both of these reactions occur in the mitochondria.

Betaine must be exported to the cytoplasm where betaine:homocysteine methyltranferase (BHMT) uses one of its methyl groups to regenerate methionine, forming dimethylglycine (DMG). This methionine can, of course, be employed for SAM production, as well as other metabolic fates (such as protein synthesis). DMG can be transported into the mitochondria, where three sequential enzymatic reactions remove its three carbons sequentially. Specifically, DMG dehydrogenase converts DMG to sarcosine, followed by sarcosine dehydrogenase which converts sarcosine to glycine(*24*).

13
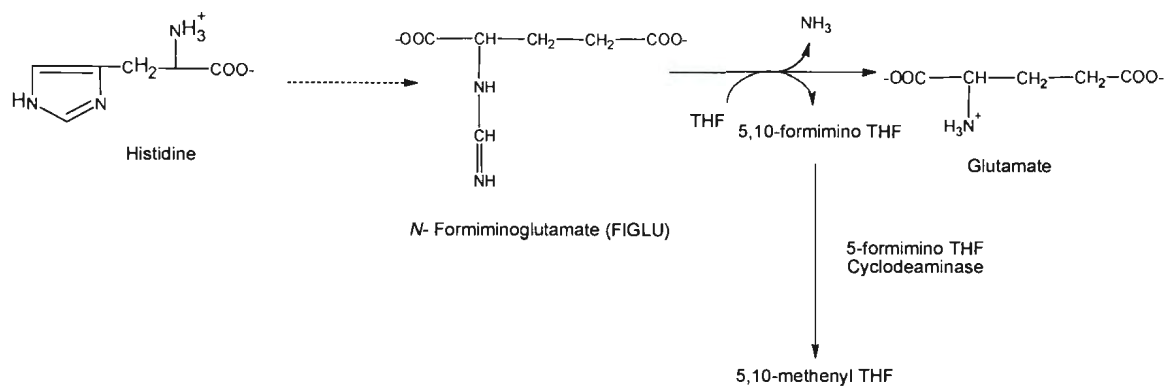
Figure 1.5. Histidine catabolism yields a one-carbon group by the conversion of N-formiminoglutamate (FIGLU) and THF to glutamate and 5-formimino THF, catalyzed by *glutamate formiminotransferase*.
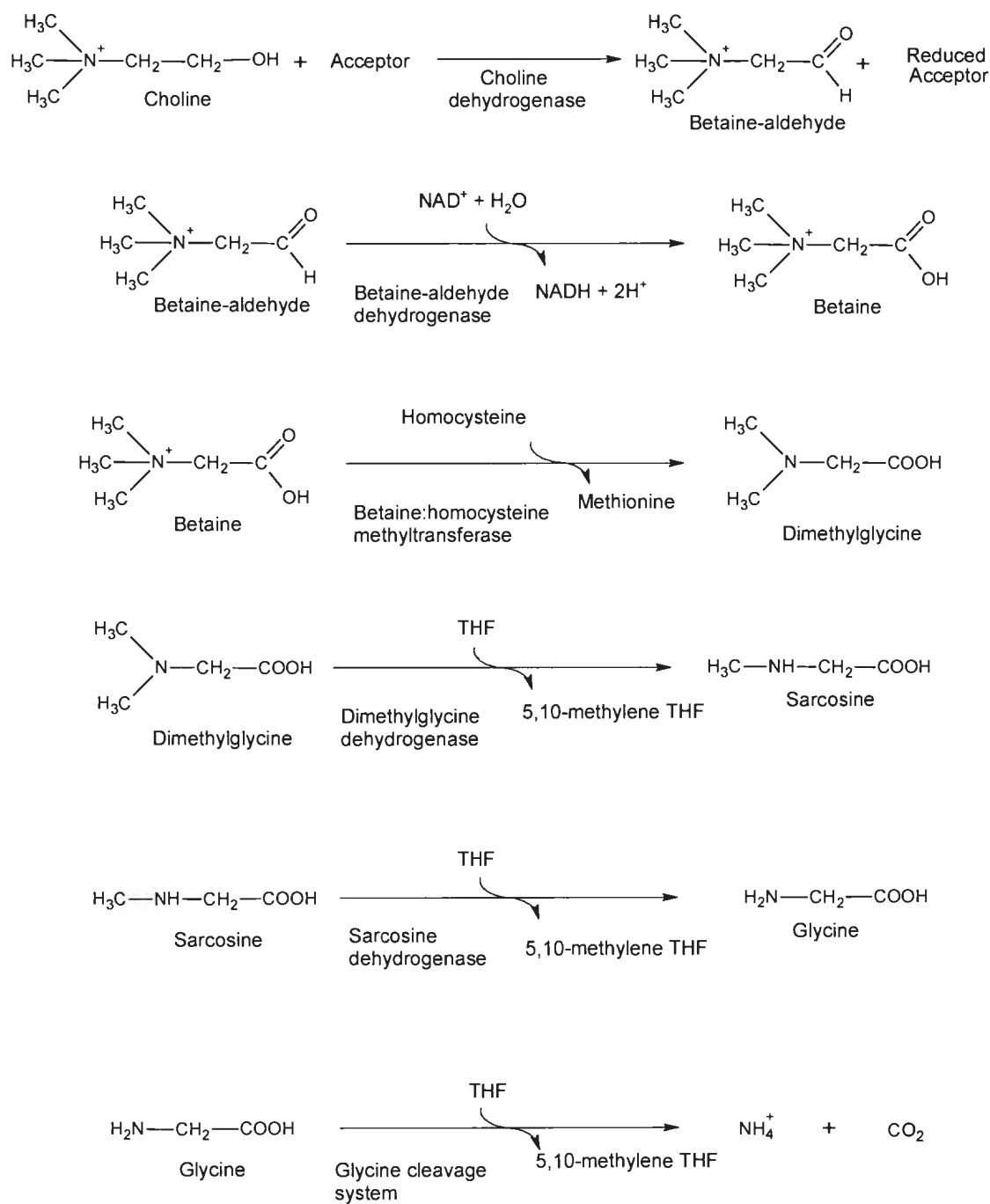
Figure 1.6. The sequence of enzymatically catalyzed reactions in the catabolic pathway for choline and subsequent metabolites (*18, 27*).

Finally glycine is catabolized to ammonia and carbon dioxide by the glycine cleavage system (described in detail in Section 1.4.2)(*18*). Each of these reactions requires THF as a co-substrate and produces a mitochondrial molecule of 5,10-methylene THF.

1.5 Folate-independent one-carbon production

A number of metabolic processes can yield free formate independent of THF. These include the catabolism of tryptophan, the α-oxidation of branched chain fatty acids, cholesterol biosynthesis, and the metabolic removal of methanol. This formate can then be incorporated into the folate-bound one-carbon pool by 10-formyl THF synthetase (located in both mitochondria and cytoplasm), and can be shuttled on to various fates(*25*).

1.5.1 Tryptophan

Tryptophan catabolism involves a step where a formyl group is cleaved in a folate-independent manner to produce formate (see Figure 1.7). Tryptophan is oxidized by tryptophan dioxygenase to *N*-formylkynurenine, which is subsequently converted to kynurenine and formate by kynurenine formamidas*e* (*26*).
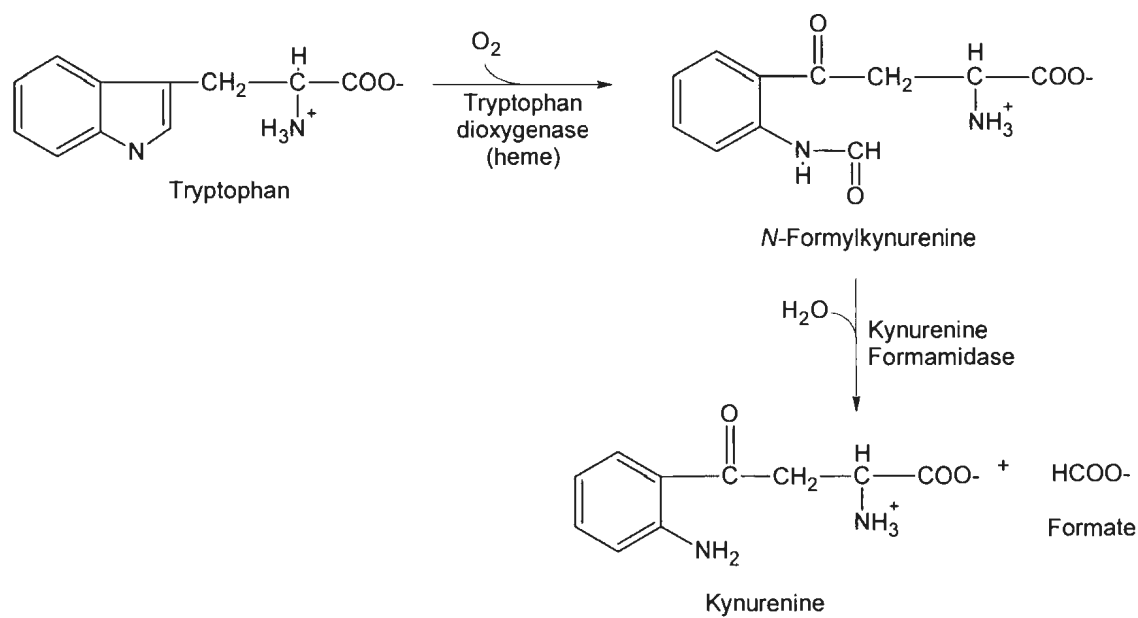
Figure 1.7. Tryptophan catabolism in the cytoplasm yields free formate.

1.5.2 Other sources of folate-independent formate

There are a number of other reactions that can produce one-carbon groups that do not feature the catabolism of precursors such as amino acids and choline. This includes the production of cholesterol (27 carbons) from its precursor lanosterol (30 carbons), during which one of the supernumerary carbons is released as formate (*28*). Another pathway that is responsible for formate production is the metabolism of branched chain fatty acids through α-oxidation(*29*); this occurs in peroxisomes. Any organism consumes vegetable matter ingests phytanic acid, the branched chain fatty acid responsible for anchoring chlorophyll in chloroplast membranes. Lastly, methanol will be metabolized to formaldehyde and subsequently to formate by alcohol dehydrogenase and formaldehyde dehydrogenase respectively (*30*).

1.6 Mitochondrial one-carbon production and utilization

As previously discussed, the mitochondrial one-carbon pool is provided by the catabolism of choline, serine, methionine and glycine. Each of these produces one or more 5,10-methylene THF units. Since one-carbon units are utilized in the cytoplasm, the mitochondrial 5,10-methylene group on THF must first be converted to free formate for export across the inner mitochondrial membrane. The release of free formate is facilitated by *C1-THF synthase*, a trifunctional enzyme which is responsible for the two-step process which results in the production of 10-formyl THF (*25*). Initially, *5,10-methylene THF dehydrogenase* oxidizes 5,10-methylene THF to 5,10-methenyl THF (accompanied by the reduction of $NADP^+$ to NADPH). This is followed by the conversion of 5,10-methenyl THF to 10-formyl THF by the action of *5,10-methenyl THF cyclohydrolase.*

The release of formate from 10-formyl THF is catalyzed by *10-formyl THF synthase*, a third component of the trifunctional C1-THF synthase(*31*). This produces one ATP in the process. Alternatively, in the presence of $NADP^+$, 10-formyl THF dehydrogenase can release the carbon as carbon dioxide, in a reaction that may serve to remove excess one-carbon potential. Once produced, formate can be transported out of the mitochondria, while the THF will be reused as a co-substrate in another mitochondrial one-carbon producing reaction. Figure 1.8 provides an illustration of the important reactions described above.

1.7 Cytoplasmic one-carbon production and utilization

The cytoplasmic one-carbon pool is more complex than the mitochondrial pool because it entails both the production and utilization of one-carbon groups, the import and export of one-carbons, as well as the inter-conversion of a number of different forms of THF-bound, one-carbon units. Figure 1.9 provides an overview of some of these processes.

Free formate, produced in mitochondria from the catabolism of serine, glycine, methionine and choline can be imported into the cytoplasm(*4*). This formate can also be supplemented by a number of folate-independent, one-carbon producing reactions that yield formate (as previously discussed) such as tryptophan catabolism, methanol metabolism, α-oxidation of branched chain fatty acids.

Figure 1.8. Catabolic pathways for dietary one-carbon precursors that contribute to to the mitochondrial one-carbon pool. The mitochondrion is shaded a light gray and dietary one-carbon precursors are surrounded by a rectangle. A box surrounds the three enzymatic activites making up the trifunctional C1-THF synthase.

Enzyme Abbreviations: BHMT – Betaine:homocysteine methyltransferase, CDH-Choline dehydrogenase, DDH – Dimethylglycine dehydrogenase, GCS – Glycine cleavage system, GNMT – Glycine-N-methyltransferase, SDH – Sarcosine dehydrogenase, $SHMT_M$ – Serine hydroxymethyltransferase mitochondrial, THFCH – 5,10-methenylTHF cyclohydrolase, mTHFDH – 5,10-methyleneTHF dehydrogenase, fTHFDH – 10-formyl THF dehydrogenase, THFS – 10-formyl THF synthase

Methionine

SAH   SAM

Sarcosine ← Glycine
         GNMT

THF   THF

DMG → DMG *DDH* Sarcosine *SDH* Glycine

Methionine   THF

BHMT   *GCS* $CO_2 + NH_3$ *SHMT$_M$*

Hcy

Methylene-THF   THF

Betaine ← Betaine Aldehyde   Serine

mTHFDH   NADP$^+$

NADPH

CDH

Methenyl-THF

Choline

THFCH H_2O

H$^+$

Formyl-THF   NADP$^+$ NADPH CO_2

ADP + Pi   *fTHFDH*

THFS   THF

ATP   THF

Formate

Activities of trifunctional
C1-THF Synthase

Formate

21
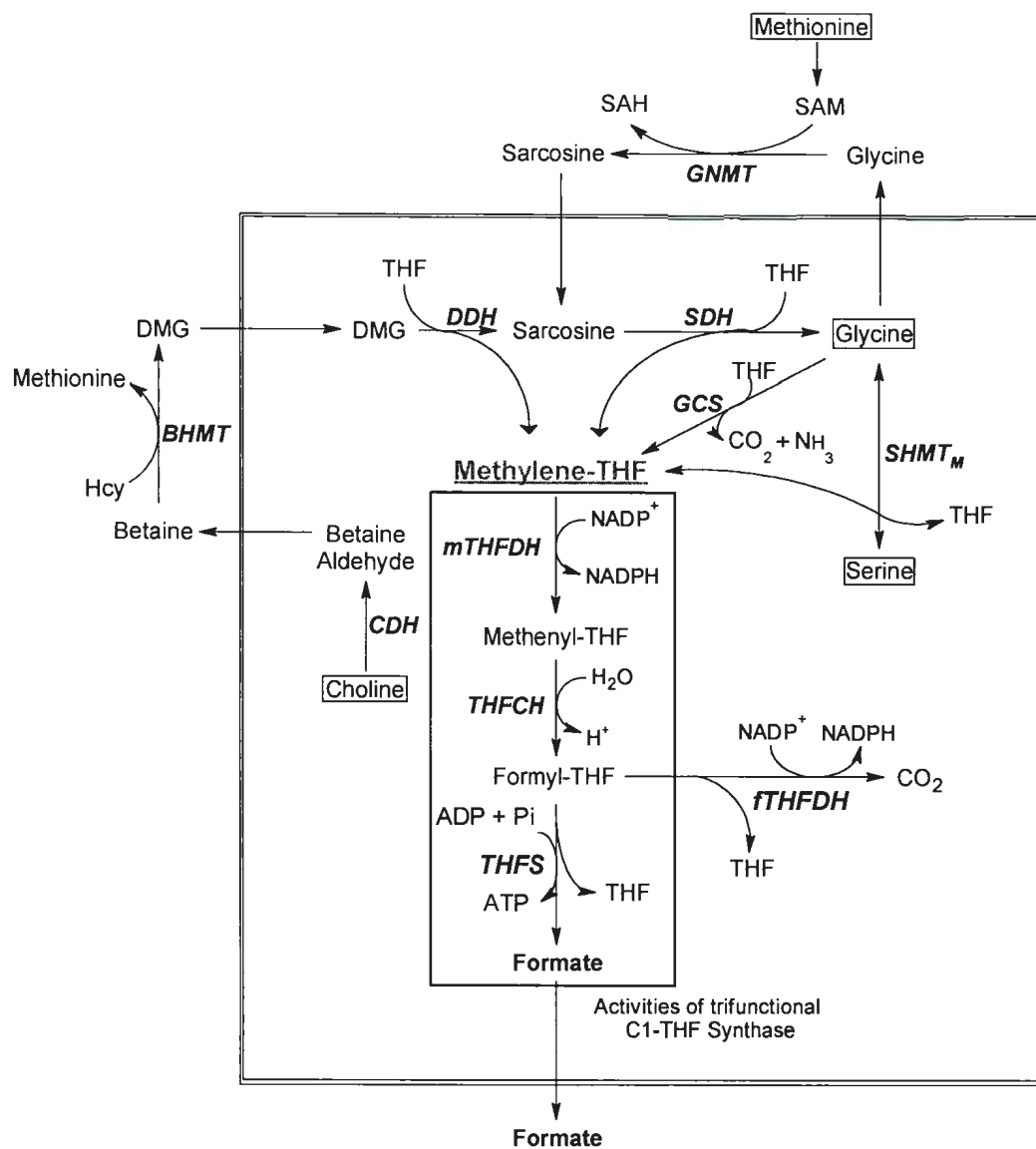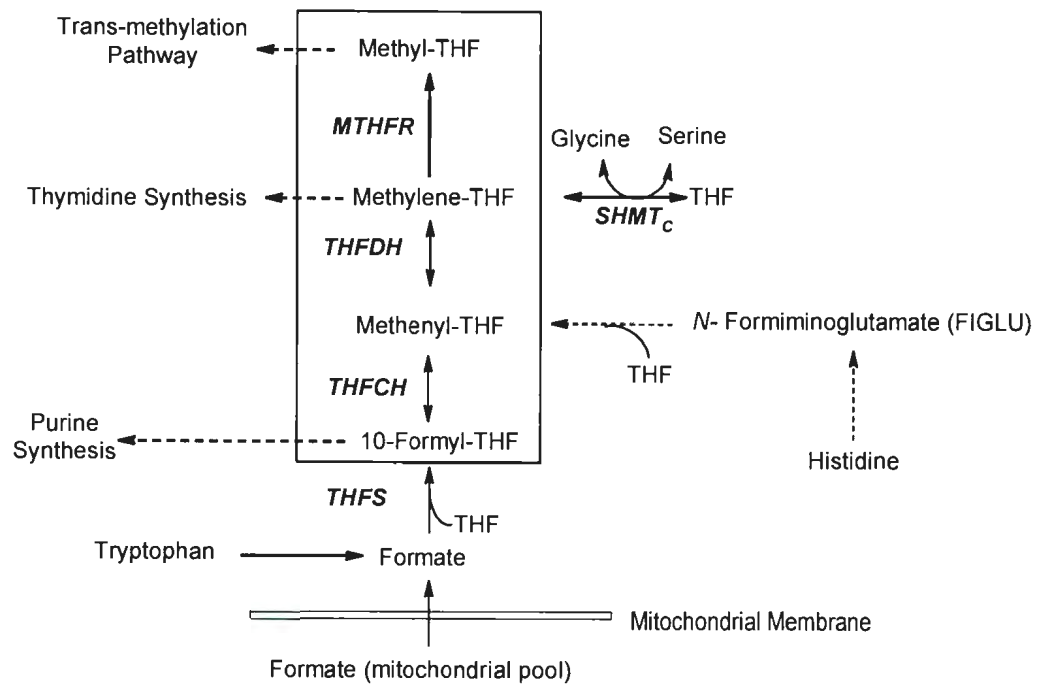
Figure 1.9. Dietary one-carbon precursor catabolism pathways contributing to the cytoplasmic one-carbon pool, and pathways requiring one-carbon groups. A box surrounds the three enzymatic activities making up the trifunctional C1-THF synthase.

Enzyme Abbreviations: MTHFR – 5,10-methylene THF reductase, SHMT$_C$ – Serine Hydroxymethyltransferase $_{cytoplasmic}$, THFCH – 5,10-methenylTHF cyclohydrolase, THFDH – 5,10-methyleneTHF dehydrogenase, THFS -10-formyl THF synthase

Some of the formate will be used by the organism for constructive purposes following integration into the folate-bound cytoplasmic one-carbon pool. 10-formyl THF synthetase converts formate and THF to 10-formyl THF. This action is one of three functional domains of the C1-THF Synthase enzyme, which also contains 5,10 methylene THF cyclohydrolase and 5,10-methenyl dehydrogenase. These functional domains allow for the interconversion of 10-formyl THF to 5,10-methenyl THF, and 5-10 methenyl THF to 5,10-methylene THF respectively. 5,10-methylene THF can be reduced one step further to 5-methyl-THF by NADPH , a reaction catalyzed by 5,10-methylene THF reductase. Pathways requiring one-carbon groups will use one of the four THF structures mentioned. One-carbons fated for methyltransferases will be fed into the transmethylation cycle via 5-methyl THF's remethylation of homocysteine to methionine (*21*). Purine synthesis requires two formyl groups from 10-formyl THF to provide C2 and C6 of the purine molecule (*32*). Thymidylate (dTMP) is created from dUMP by the action of thymidylate synthase, a reaction requiring 5,10-methylene THF as the substrate (*33*).

1.8 Removal of formate

Metabolic activity is linked to the production of reactive oxygen species such as hydrogen peroxide. (*34*) Among an organism's general defenses against oxidative damage is the enzyme *catalase*. *Catalase* is among the most active and ubiquitous enzymes in the biosphere, responsible for the removal of hydrogen peroxide via a dismutative mechanism. A secondary function of *catalase* is the peroxidizing

decomposition of various hydrogen donors (such as formic acid), which occurs in

the presence of a corresponding quantity of peroxide (see equation 1).

$$H_2O_2 + COOH_2 \rightarrow 2H_2O + CO_2 \tag{1}$$
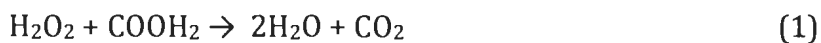
This secondary activity of *catalase* provides another mechanism for the removal of

excess one-carbon units from the cell.

In addition to catalase, a number of other significant mechanism exist which

clear formate. Formate may be oxidized to carbon dioxide, which may be then

removed from the body by gas exchange in the lungs. This occurs both in the

mitochondria as well as in the cytoplasm. Mitochondrial-derived formate can also

be exported to the cell where it may be incorporated into the cytoplasmic 1C

pool(*12*).

1.9 Historical viewpoints of one-carbon metabolism
Literature concerning the relationship between folic acid and formate begins

to appear in the late 1940s to early 1950s, mainly describing studies making use of

radiolabelled molecules (tracers). Radioactive dietary formate precursors and

radioactive formate were used to measure the relative contributions to the formate

pool and the fates of formate respectively(*35, 36*). Several points stand out as to the

difference between these historical interpretations and our contemporary

understanding of one-carbon metabolism. Although there was discussion of the

relationship between formate and folate, there is no clear indication in the early

work that folate is directly involved as a substrate and carrier in one-carbon

producing reactions (*11, 37*), nor was there a clear understanding of the relevant

enzymes as we now know them. On a similar note, while we now understand that both folate-bound and free variants are at play in the supply and utilization of one-carbon units, the early literature refers to this pool exclusively as "formate", and we find that there is no discussion of the folate being used as a carrier of one-carbon units.

Tangential work in the field of microbiology determined that inhibiting the production of p-amino benzoate (PABA, a precursor and structural constituent of folate) in *Escherichia coli* would reduce the production of purines(*38*). Plaut et al. (*37*) recognized the relationship between PABA and folate and drew the correct conclusion that folic acid was somehow involved in the production of purines. Further work determined that folate-mediated, one-carbon metabolism was responsible for incorporating the carbons at positions 2 and 8 of the purine rings (*35*). They took this a step further and noted that in those animals deficient in folate, less radioactive formate was incorporated into liver purines than those animals supplemented with folate(*35*). This work provided a link between formate metabolism and purine production without offering a specific mechanism. The authors note that folate "controls the incorporation of formate" into the purines without explicitly understanding that folate acts as the carrier of the one-carbon group.

Modern reviews of the relevant literature identify the provisioning of one-carbon units towards purine/thymidylate production and methyltransferases as the 'raison d'être' for folate-mediated one-carbon metabolism(*1*). By contrast, some

early papers were concerned with the contributions of formate towards the interconversion and production of amino acids. Early work from Plaut's laboratory centered on the incorporation of free formate into amino acids in folate-replete and folate-deficient animals (37). Although it is recognized that serine can be produced from glycine due to the bi-directional nature of SHMT, this no longer seems to be emphasized as a key factor in maintaining serine levels. In fact, modern work has tended towards the opposite, suggesting that serine catabolism (producing glycine) is the principal source of one-carbon units used to re-methylate homocysteine to provide methionine for use in the transmethylation cycle(15).

1.10 Biomedical aspects of formate

Formate plays an important clinical role in the identification and management of chronic alcohol abuse. Kapur et al. showed that the mean plasma formate levels were significantly higher in alcoholics as compared to control patients. A supplementation of THF was able to lower the plasma formate concentration and mitigate the neurotoxicity observed in control chronic alcoholics (56).

1.11 Objectives of research

The experimental work contained within this thesis contributed towards four broad aims.

1. Optimization of a coupled assay with *formate dehydrogenase* and *diaphorase* to determine plasma formate concentrations in an accurate and efficient manner. The ability to reliably assay the formate concentration of plasma was

absolutely essential for most of our work, necessitating a method that was both efficient and high-throughput. We set to work optimizing an enzyme-based spectrophotometric assay and adapting it to a microplate reader. Initial tests revealed that even after the assay came to completion, the apparent absorbance would continue to increase (non-specifically) in a linear fashion. This "creep" was eliminated following systematic testing of different tetrazolium dyes and oxidation-reduction couplers, along with the use of a miniature desalting column to remove impurities from the commercial enzyme preparations. As a result, we were able to increase the utility of the assay at minimal cost and with no increase in time.

2. Establishment of a robust model of folate deficiency in the rat. Initial work on folate-deficiency was carried out using a standard, commercial folate-deficient diet in which free amino acids replaced protein. It was observed that even on a relatively short timescale (15 days), there were apparent differences in the weight gain between folate-replete and folate-deficient animals. In order to carry out our final two objectives, we experimented with changing the diet and/or experimental timescale such that our animals were as healthy as possible while maintaining symptoms of folate-deficiency (elevated plasma formate and homocysteine). This work comprised two studies. Initially we compared plasma formate, and plasma homocysteine concentrations between the commercially-sourced amino acid-defined diet and a folate-deficient casein-based AIN-93G diet, produced in-house. After switching to the AIN-93G diet, we ran a second experiment to determine the optimal length of feeding.

3. Determination of in vivo kinetics/endogenous formate production in control and folate-deficient rats. Although early work demonstrated a difference in the "static" concentrations of plasma and urinary formate between folate-replete and folate-deficient rats, limited work has been conducted concerning the rates of production. Using a constant infusion of sodium ^{13}C-formate, we found a significant difference in rates of free formate production between healthy and folate-deficient animals. Knowing the quantities of food ingested, and the content of potential one-carbon groups in the food, we compared the relationship between ingested potential formate precursors and the rate of endogenous formate production between folate-replete and folate-deficient animals.

4. Determination of the importance of particular dietary one-carbon precursors. After determining the proper diet and timescale, we ran a series of experiments in which we increased, one at a time, the dietary concentration of a variety of known or suspected one-carbon precursors. These experiments were conducted in both healthy and folate-deficient animals. We compared the mean plasma formate and urine formate concentration in each precursor-supplementation group against their respective healthy or folate-deficient control. In those cases where there was a significant increase in plasma or urine formate excretion above the control group, we concluded that the increased formate precursor supply was responsible and that the precursor in question might therefore be an important donor to the free one-carbon pool.

Chapter 2 – Methods

2.1 Chemicals

Formate dehydrogenase (isolated from Candida Boidinii, Cat. # F8649) and pentafluorobenzyl bromide (PFBBr) were obtained from Sigma Aldrich (U.S.A), *Diaphorase* (isolated from Clostridium kluyveri) was obtained from Worthington Biochemical (U.S.A.). Sodium ^{13}C-acetate and sodium ^{13}C-formate were obtained from Cambridge Isotopes (U.S.A.). Sodium pentobarbital was obtained from Ceva Santé Animale (France). Acetonitrile (HPLC grade) was obtained from Fisher Scientific (U.S.A). Isoflurane was obtained from Abbott Animal Health (U.S.A.). Gas cylinders were procured from Air Liquide Canada, at the quality appropriate for biological use (U.S.P. grade). Unless otherwise noted, all other chemicals were procured from Sigma-Aldrich, and all solvents from Fischer Scientific.

2.2 Animal care

All studies were conducted with male Sprague-Dawley rats sourced from the Vivarium, operated by Memorial University's Animal Care Services Department. These were delivered to us shortly following weaning (4 weeks of age), were weighed and were housed individually in clear cages in a temperature and humidity controlled facility. Lighting was controlled by computer and followed a twelve hours on, twelve hours off routine (7AM lights on,7PM lights off). Animals were fed one of two purified experimental diets, depending on the particular experiment (these are described subsequently). Blood and tissue samples were taken from anesthetised rats (sodium pentobarbital i.p., 5.5 mg/100g body weight). For the constant infusion experiments, rats were anesthetised with isoflurane in oxygen (induced at 4%, maintained at 2%) using U.S.P. grade oxygen as the carrier gas. All

animal protocols were approved by the Institutional Animal Care Committee of Memorial University of Newfoundland and were in accordance with the Guidelines of the Canadian Council on Animal Care.

2.3 Preparation of diets

Two diets were employed in this work, both of which were used to induce moderate folate-deficiency in our experimental animals. The first is an amino acid-defined diet produced commercially by Dyets Inc (Bethlehem, PA), (folate deficient - #517777, folate-replete - #517802). It was a modified (39) version of Clifford-Koury's original folate-deficient diet (40). The second diet was a growth-enabling form of the rodent casein-based diet endorsed by the American Institute of Nutrition, known as AIN-93G (41). The amino acid profiles of these diets were compared in Appendix B. The compositions of both diets were included in Appendix C. These diets were modified to allow both folate-replete and folate-deficient forms of the respective diets.

With the exception of amino acids and the following specific components, all dietary ingredients were sourced from MP Biomedical (formerly ICN), a corporation which markets chemicals specifically for use in research diets. Mineral mixes and vitamin mixes were obtained from Dyets Inc. Tert-butylhydroquinone was obtained from Sigma-Aldrich.

In the course of conducting precursor supplementation studies, we increased particular known and suspected one-carbon precursors at the expense of other ingredients. These additions accounted for, at most, around one percent of the total

diet. The commercial amino acid-defined diet (Dyets) came premixed, so all other ingredients were scaled back according to how much precursor we wished to supplement. When we switched to the AIN-93G diet, which we prepared in-house from separately sourced ingredients, we were able to offset precursor addition through the reduction of specific ingredients. Since corn starch was present in the greatest quantity, it was scaled back according to the mass of the 1C precursor supplemented in a particular diet. These modifications are discussed as they arise.

Our Dyets Inc. diets were analyzed in the lab of Dr. MacFarlane (Ottawa) of Health Canada to determine their folate content. This analysis employed a microbiological assay using Lactobacillus Casei grown in a medium lacking folic acid(42). The general principle was that the turbidity of the final culture would be proportional to the extent of *L.Casei* proliferation, which would depend directly on the quantity of folate present in the diet sample.

2.4 Collection of urine

Urine collection always took place on the penultimate day of a study, or one day prior to blood and tissue sampling. Animals were placed in metabolic cages in the morning, and the urine collection tube was spiked with 25 µL of 80 mM sodium azide to act as a preservative (43). Collection ran for 24 hours.

2.5 Collection of blood

Following induction of anesthesia, rats were dissected so as to expose the peritoneal cavity (from below the intestines to just below the diaphragm). At all times, great care was taken not to puncture or disturb the chest cavity. Saline-soaked gauze was used to expose the abdominal aorta. Approximately 3mL of blood

were taken into a heparinized syringe. This blood was stored in glass tubes on ice, then centrifuged at 1800 RPM (550g) for 10 minutes to separate the plasma which was subsequently stored in 1.5 mL aliquots at -80° C.

2.6.1 Plasma formate concentration (*formate dehydrogenase /diaphorase*)

The enzymatic formate assay is based on a coupled enzymatic reaction involving *formate dehydrogenase* (FDH) and *diaphorase* (see Figure 2.1). It was designed as a traditional spectrophotometric assay (*44*), but we optimized it for microplates . The basic reagents were unchanged, but their concentrations varied and total assay volume was less. FDH oxidized formate to CO_2 while simultaneously reducing NAD^+ to NADH. Diaphorase then recycled NADH back to NAD^+ while simultaneously reducing iodonitrotetrazolium chloride (INT) to its formazan dye which had a peak absorbance at 500 nm. Thus, the change in absorbance was directly proportional to the amount of formate in the original sample.

A series of samples containing HPLC-grade water (instead of plasma) were run in conjunction with our analytical samples in order to allow us to account for any formate present in our reagents. This value was deducted from all analytical samples and spiked analytical samples prior to any calculations. In addition to controlling for reagent-based formate, we also accounted for any non formate-specific absorbance at 500 nm. To account for absorbance at 500 nm that is not attributable to formate oxidation, we ran our assay in the absence of FDH until an initial plateau was reached. Following the addition of FDH, we calculated the increase in absorbance and used this to calculate the formate concentration. When our lab began using this assay we noted that, for similar concentrations of formate, aqueous standards reached a plateau faster than plasma samples.

33

Formate   Formazan Dye

Formate
Dehydrogenase

NAD$^+$ + H$^+$

Diaphorase

NADH

CO_2 Iodonitrotetrazolium
                (INT)
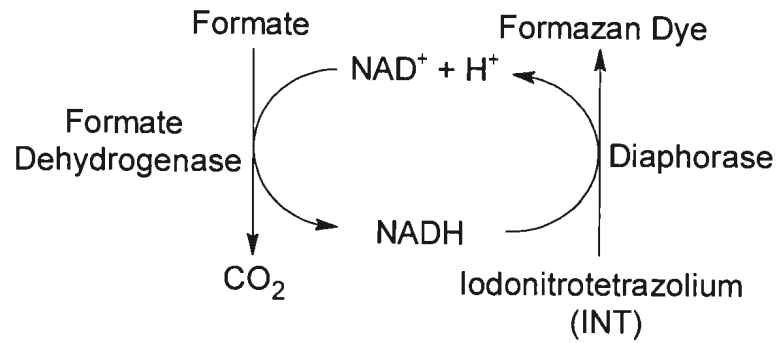
Figure 2.1 The two step enzymatic reaction involved in the enzymatic formate assay. For each formate oxidized to carbon dioxide, one molecule of INT was reduced to a formazan dye, the absorbance of which could be measured at 500 nm.

To eliminate any inconsistency, we decided that a plasma-based standard would be required. This was accomplished by spiking analytical samples with a known amount of formate. In such cases, a small amount of 10 mM sodium formate solution was added to acetonitrile.

For each biological sample, two unique deproteinizations using HPLC-grade acetonitrile were conducted. One of these used unspiked acetonitrile, while the other used the spiked acetonitrile. The unspiked sample was run in triplicate, while the spiked sample was run alone. The averaged absorbance corresponding to the unspiked triplicates was subtracted from the spiked sample, to determine the absorbance corresponding to the known quantity of formate in the spike. On each microplate, we averaged all the spike absorbance values to calibrate the biological unknowns on each plate by way of a one-point calibration. We then solved for the unknown concentration in each normal analytical sample (based on the triplicates).

Briefly, the procedure was as follows: Plasma was deproteinized by the addition of an equal volume of acetonitrile. Analytical samples were deproteinized with HPLC-grade acetonitrile; for spiked samples we used a mixture containing 95% HPLC-grade acetonitrile and 5% 10 mM sodium formate in HPLC-grade H2O (vol/vol). (This meant that each spiked sample had a concentration equivalent to the unknown analytical sample plus 0.25 mM formate.) Following two successive rounds of centrifugation (15000 x g, 10 min each, carrying over supernatant to second round), 50 µL of the clear supernatant was added to 200 µL of phosphate buffer cocktail (pH 7.4, 0.1 M) containing INT (1 mg/mL), NAD+(1 mg/mL) and

diaphorase (0.8 U/mL). INT was added first and stirred vigorously for one hour to ensure complete solubility. NAD$^+$ and diaphorase were added subsequently; five minutes prior to initiation of the assay and stirred gently. After monitoring the absorbance (500 nm) for several minutes to ensure a plateau, 10 uL of FDH was added (15 U/mL). Low molecular weight contaminants in FDH were removed by passing the solution through a PD-10 desalting column before use in the assay. The absorbance was recorded for ~2 hours, until a plateau was reached. A separate experiment determined that a linear response was obtained over the expected range of plasma formate concentrations expected from folate-replete and folate-deficient animals (up to 1 mM).

2.6.2 Plasma formate concentration (GC-MS)

A gas chromatograph in conjunction with a mass spectrometer (GC-MS) was used previously to measure the formate concentration in plasma samples (45). A known quantity of "heavy" sodium ^{13}C-formate was added as an internal standard prior to derivatization by pentafluorobenzyl bromide (PFBBr). The unlabeled formate appeared at 226 m/z, while the heavy formate appeared at 227 m/z (1 amu higher). The ratio of peaks allowed for a determination of the plasma formate concentration. A standard curve was run with each assay, covering the expected formate concentration range for plasma in folate-replete and folate-deficient rats to confirm linearity in the assay.

When we examined the peak 1 m/z above the regular formate peak (227 m/z), it was important to bear in mind that there was naturally occurring ^{13}C and ^{2}H present beyond that which existed in the form of the ^{13}C-formate internal standard.

These naturally occurring isotopes were present in both the derivitizing agent as well as in the endogenous formate sample. For a natural sample of formate, the 227 m/z peak was 8.7% of the magnitude of the 226 m/z peak.

2.6.3 13C-formate enrichment (GC-MS)

Our studies of in vivo formate kinetics required the infusion of sodium ^{13}C-formate into the blood of an experimental animal. Periodic blood samples were then taken in order to monitor the ratio of the artificially-introduced heavy formate to endogenous formate produced by the animal. This posed a challenge; since sodium ^{13}C-formate was infused during the experiment, it could not also be used as the internal standard during analysis.

To overcome this challenge, we introduced another simple carboxylic acid, (acetate) which is derivitized similarly to formate. Since acetate will occur naturally in biological samples (at varying concentrations), sodium ^{13}C-acetate is introduced as the internal standard. The absolute formate concentration was determined by comparing the area under the peaks corresponding to regular formate and heavy acetate (226 m/z and 242 m/z respectively). Next, the ratio of artificially-introduced heavy formate to endogenous formate is calculated as the ratio of peak areas for 227 m/z to 226 m/z. This is referred to as the tracer: tracee ratio or TTR.

The assay was run by combining 15 µL of buffered internal standard (1mM sodium 13C-acetate in 0.5 M pH 8.0 phosphate buffer), 35 µL of plasma and 93 µL of PFBBr (100 mM in acetone). Following one minute of vortexing in screw top glass vials, the samples are incubated for 15 minutes at 60° C. After 2 minutes on ice, 233

μL of hexane was added, followed by another minute of vortexing. Two separate layers formed, the top consisting of an organic phase, and the bottom consisting of the aqueous phase and protein. The organic phase was carefully separated and run on the GC-MS (Thermo-Fisher Scientific 'Trace GC Ultra', carrier gas - 99.9997% pure methane,) using a splitlesss mode(ratio of 10, 1.5 minutes). The autosampler injects 1μL onto a 0.32 mm x 30 m Agilent DB225 MS column. The run begins at 40° C, and increases by 15° C/min to 140° C, then increases at a rate of 50° C/min to 240° C. The full run lasts for 13.67 minutes. The MS uses EI-SIM mode(Electron Impact- Single Ion Monitoring), which exclusively monitors the mass fragments at 226, 227 and 242 m/z. These correspond to formate, ^{13}C-formate and ^{13}C-acetate respectively.

2.7 Formate concentration in urine (proton NMR)

Samples were thawed, vortexed and mixed 9:1 with 1.5 M phosphate buffer and finally syringe filtered through 0.45μM filters (12). This mixture was inserted into 5 mm thin-walled 600 MHz-rated NMR tubes from Wilmad Glass. A coaxial insert (0.2 mM DSS in D_2O) was loaded into the centre of each tube to calibrate and lock the signal. 256 scans were run on each sample, using a Bruker Avance 600 MHz NMR spectrometer, with a TXI probe at a temperature of 298 K. The pulse program used a water-peak suppression program, producing a formate peak at 7.39 ppm relative to the DSS peak. The ratio of this peak to the DSS peak (appearing at 0 ppm) was proportional to the concentration of formate in the sample. Before running analytical samples, a standard curve was run on a series of standards to ensure linearity of the assay and allow for quantification of formate concentration. The use of the peak ratio (as opposed to absolute size of formate peak) accounts for any day-to-day variation of the assay.

2.8 Measurement of urinary creatinine

Urinary creatinine was measured by the method of Yuen et al.(46) without any modifications. A Waters HPLC system was employed with a Hamilton PRP X200 cation-exchange column.

We normalized the urinary excretion of formate to the urinary excretion of creatinine. Creatinine is produced by the non-enzymatic breakdown of the body's pool of creatine. This occurs at a rate of 1.7% of the total pool per day in humans(47). The use of creatine as a marker of urine excreation assumes that it is a valid marker of GFR, and that the conversion of creatine to creatinine is the same under all physiological and pathological conditions. Since the creatine pool is maintained at a constant level, normalization to creatinine excretion allowed for an unbiased comparison of urinary metabolite excretion between experimental groups (such as from differences in the urine concentrating activity in kidney, or incomplete urine collections) (48).

2.9 Catalase activity

Catalase activity was measured in liver samples according to the method of Aebi et al. (34). Liver was flash frozen using clamps cooled in liquid N_2. Prior to analysis of experimental samples, we ensured that activity determinations were linear with respect to quantity of liver assayed and time of assay.

2.10 Homocysteine in plasma by HPLC

Total homocysteine in plasma was analyzed by the method of Vester and Rasmussen(*49*) with one modification. The internal standard was 8-aminonapthalene-1,3,6-trisulfonic acid (ANTS) in place of mercaptopropionyl-glycine. This was run on a Shimadzu HPLC system equipped with fluorescence detection on a Hypersil ODS (5µm) column.

2.11 Statistics

Simple statistical analyses, consisting of two data sets were, were conducted using two-tailed t-tests. A one-tailed t-test was used in those cases where similar previous data (either from the literature or from our own work) existed which could be used to predict a outcome. A significant result was accepted as $P \leq 0.05$.

Experimental designs consisting of multiple groups were analyzed using one-way ANOVAs, with pre-defined a priori comparisons against a control group. These multiple comparisons were conducted with Dunnett's test (which is designed for one-way ANOVAs in which several treatment groups have to be compared aginst a control group). The analysis of these is described in more detail as they arise.

T-tests were conducted using Prism 3 for Windows. ANOVAs and multiple comparisons were conducted using R statistical programming language.

Chapter Three - Optimization of a coupled assay with formate dehydrogenase and diaphorase for determining plasma formate concentrations

3.1 Experimental Approaches

The procedure for the measurement of plasma formate using the coupled-enzyme system was aimed at increasing the sensitivity of the assay to formate, while reducing the background noise.   Earlier work by our lab succeeded in modifying the assay from a traditional spectrophotometer setup (utilizing 3 mL cuvette) (*44*) to microplates. The major advantages of the microplate are the ability to read many samples in tandem, as well as the use of much less plasma. It was noted that even after completion of the assay, the absorbance would continue to rise in a linear fashion (this was termed "the creep").

The assay was optimized in a number of ways:

1) We suspected the presence of a thiol additive in the enzyme preparation due to the smell. A literature search revealed that commercial preparations of FDH often include the use of the reducing agent dithiothreitol (DTT) (*50*). In order to eliminate any non-specific reduction of the tetrazolium dye due to DTT contamination, we ran the FDH preparation through a desalting column to remove small molecules.

2) We determined the best type of tetrazolium dye for the assay.

3) We determined the relative usefulness of an enzyme coupler (*diaphorase*) versus a chemical coupler to link the oxidation of formate to the reduction of the tetrazolium dye.

3.2 Results

Buffered FDH solution was prepared (15 enzyme U/ml in 100 mM phosphate buffer, pH 7.4), and applied to a commercial PD-10 desalting column (purchased from GE Healthcare). The column works on the basis of size exclusion, with larger molecules (i.e. proteins) being eluted prior to smaller molecules. FDH was prepared according to the "gravity protocol" included with the columns. According to the manufacturer, the eluate retains 95%+ of the proteins while eliminating close to 100% of any salts or small molecules. By Sigma Aldrich's definition, one enzymatic unit of FDH will oxidize 1.0 μmole of formate to CO_2 per min in the presence of β-NAD at pH 7.6 at 37 °C.

Six samples were taken from a pool of rat plasma. They were deproteinized with acetonitrile and prepared as previously described (Section 2.6.1). Unfiltered FDH solution was applied to three of these samples, while gel-filtered FDH solution was used on the remaining three samples. The absorbance at 500 nm was monitored for 2 hours (one minute intervals). Results are given in Figure 3.1. Using the crude enzyme preparation (regular FDH), there was a continuous creep in the spectrophotometric reading so no result could be obtained. When small molecules were removed (gel-filtered FDH), the assay came to completion and a reliable reading could be obtained.
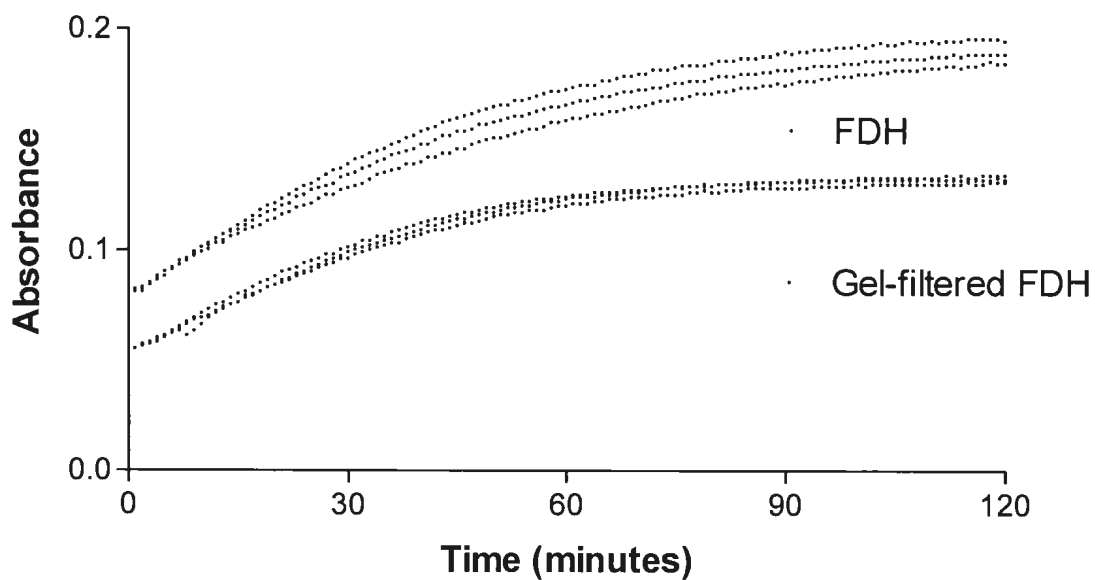
Figure 3.1. A comparison of a deproteinized plasma (with diaphorase, NAD+, and

INT) after addition of both standard *formate dehydrogenase* (FDH) preparation and a

FDH preparation gel-filtered using a PD-10 desalting column.

We conducted trials to determine if we could make the assay more sensitive by using a tetrazolium salt with a higher extinction co-efficient. A new tetrazolium dye, 2-(4-iodophenyl)-3-(4-nitrophenyl)-5-(2,4-disulfophenyl)-2H-tetrazolium (marketed as water soluble tetrazolium-1; WST-1) was obtained from Dojindo Chemical (Japan) (*51*). WST-1 was tested in conjunction with the chemical coupler methoxy 5-methyl phenazinium methylsulfate (PMS) to couple the NADH to the reduction of the dye (the chemical coupler was used in place of *diaphorase*). WST-1 was specifically engineered to be readily water-soluble due to the addition of two hydrophilic sulfide groups. Both WST-1 and INT were tested on a series of aqueous formate standards (0, 16 and 24 µM) using desalted FDH. The INT/*diaphorase* system was run as per the previous procedure (Section 2.6.1). The WST-1/PMS buffer cocktail contained PMS (20 µg/mL) and WST-1 (1 mg/mL) in place of *diaphorase* and INT respectively. The NAD^+ and phosphate buffer concentrations remained unchanged. These particular dye-reduction coupled systems were chosen from literature data (*44, 51*).

Figure 3.2 shows a set of aqueous formate standards run with the two different dye-reduction systems. Although the absorbance is higher for the WST-1/PMS dye-reduction system (due to a higher extinction co-efficient), there is the

(a) Iodonitrotetrazolium (INT) Dye with Diaphorase
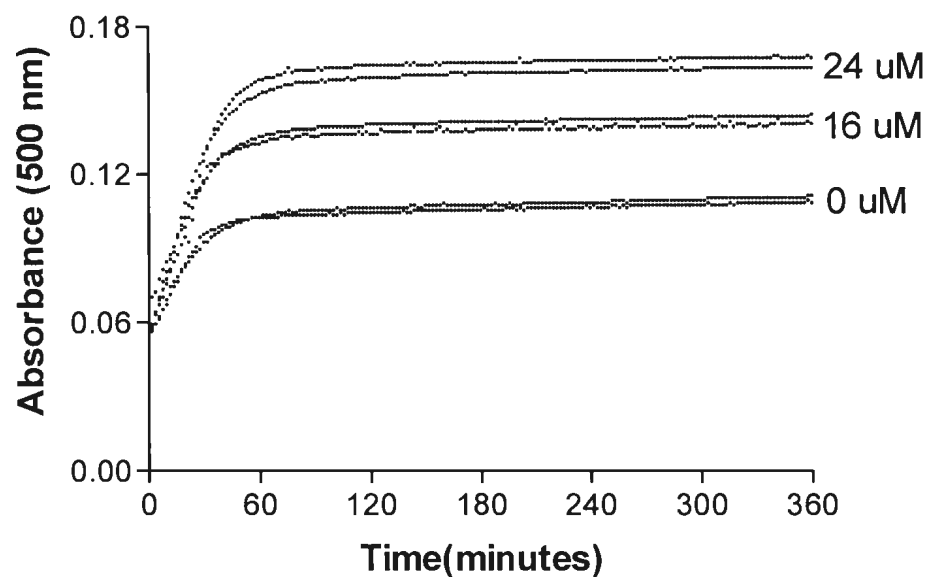
(b) Water Soluble Tetrazolium-1 (WST-1) Dye with PMS
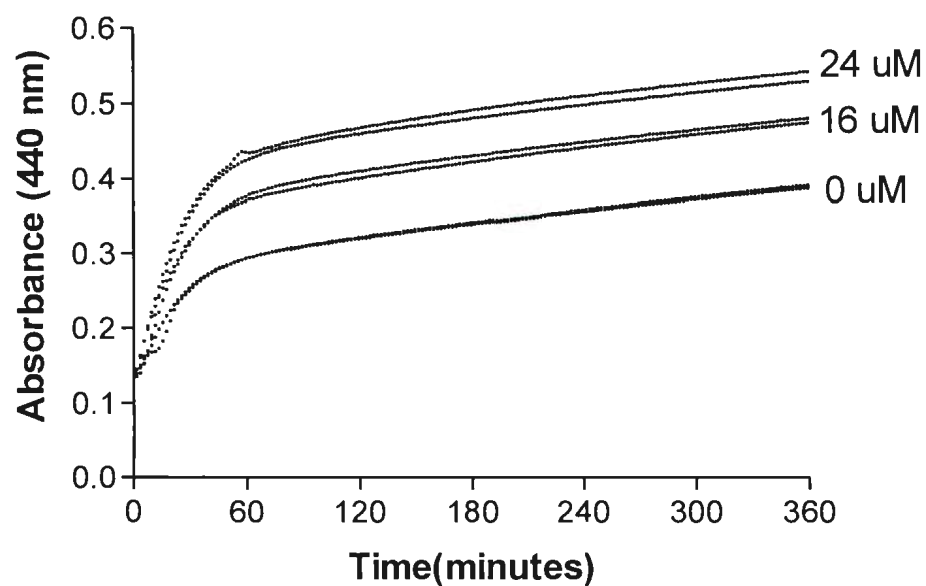
Figure 3.2.   A comparison of a set of aqueous formate standards measured by two dye-reduction systems.

enormous drawback of the lack of a stable plateau. This is suggestive of NADH-independent reduction of the dye.

3.3 Analysis

On the basis of the data shown in Figure 3.1, the desalted FDH was superior. The variability of replicate samples lessened, but more importantly, the stable plateau provided a reliable determination of formate. This cannot be said for the untreated FDH preparation as the absorbance continued to "creep".

The data provided in Figure 3.2 led us to choose the INT/*diaphorase* dye-reduction system. The deciding factor in this case was that the WST-1/PMS system introduced a noticeable "creep", which would not permit accurate determinations of formate concentrations. Although the sensitivity of the WST-1/PMS system was superior, we could still detect concentration differences of ~5 µM using the INT/diaphorase system. Given that the folate-replete animals have a baseline plasma formate concentration of ~50 µM, and moderate folate deficiency increases this several-fold, we found that this sensitivity was quite suitable for our purposes.

Chapter Four– In vivo kinetics; rates of endogenous formate production in control and folate-deficient rats

4.1 Introduction

In order to understand the differences in formate levels, we needed to be able to quantify the underlying rates of endogenous formate production. An analysis of plasma formate concentrations does not provide any information on the underlying kinetics of formate production. The use of isotopic tracers allowed us to determine the rate at which the rat produces formate (*52*).

4.2 Stable Isotopic Tracers

The biological molecule of interest is defined as the tracee (*52*). A corresponding tracer is employed, which is essentially the same molecule, but with one of its constituent atoms being an isotope with a higher or lower atomic weight than that which is naturally abundant. In our experiment, ^{13}C-formate and ^{12}C-formate acted as tracer and tracee respectively. These two molecules are known as isotopomers and, although metabolically indistinguishable within the rat, differ by 1 amu. On this basis, a gas chromatograph equipped with mass spectrometer (GC-MS) was used to differentiate between, and quantify, these formate isotopomers. A key assumption of this method is that the tracer be metabolically identical to the tracee. It was also important that the supply of exogenous tracer did not overwhelm the endogenous formate. If the artificially introduced formate pushed the concentration beyond normal physiological ranges, the experiment could not be considered to be representative of the natural state of the rat.

Stable isotopic tracer methodology involves the infusion of the tracer into the rat, at a known and constant rate, for several hours. After some time, the tracer and tracee come to an equilibrium, due to the dilution of tracer by endogenously

produced formate. The next challenge is determining the extent of the whole body

pool of tracee to which the tracer will have unhindered access. In order to track the

movement of tracer mathematically, the organism is modelled as one or more

compartments, within which the tracer and tracee can move freely. We have

therefore made use of the single compartment model to describe the movement of

tracer within the rat's endogenous formate pool. It is assumed that an equal tracer

to tracee equilibrium is reached simultaneously throughout the entire organism.

The tracer to tracee ratio (TTR) is used to describe the steady-state isotopic

enrichment. The confirmation of a plateau is based on a series of measurements of

^{13}C- and ^{12}C- formate in plasma and, along with our rate of tracer infusion, allows us

to calculate the endogenous rate of formate appearance (production) as follows:

$$Ra = \frac{R_{inf}}{E},$$

where Ra is the endogenous rate of appearance(μmol/hr) of formate in the rat, R_{inf}

is the rate of infusion of sodium ^{13}C- formate (μmol/hr), and E is the plateau TTR

(after equilibrium has been attained). This equation requires that both the TTR and

metabolite concentration be stable.

4.3 Procedure
We determined the endogenous production rate of formate for six rats fed a

folate-replete diet (Dyets #517802) and six rats fed a folate-deficient diet (Dyets

#517777) for fifteen days. In preliminary experiments, we established that fifteen

days provided a robust state of folate-deficiency, while still allowing the animal to

grow. Initial weights and specific growth rates (over final four days) are in Table 4.1. Figure 4.1 provides the growth curves for rats in this experiment.

With the aid of previous work concerning the endogenous production of formate in sheep (53), we aimed for a steady-state TTR of ~10%. The stock labelled sodium ^{13}C-formate solution of 150 mM (300 mOsM) was diluted with 0.9% saline to give an infusate with a final concentration of 12.4 mM. This was filtered through a 0.2 μm syringe filter before infusion. A 5 mL Hamilton Syringe and Harvard Microliter syringe pump (setting 6) provided ~700 uL (8.8 μmol of sodium ^{13}C-formate) per hour without a priming dose. The rate of infusion was calculated to replace the fluid losses due to blood sampling.

Rats were anesthetized with isoflurane in oxygen (4% for induction, 2% for maintenance) and catheters were surgically implanted into the femoral artery and contralateral femoral vein, and secured by silk suture. Catheters were produced by connecting a 4 cm length of PE-50 tubing to 12 cm of thinner PE-10 by heat adhesion. The sodium ^{13}C-formate/saline solution was infused via the venous catheter, and blood samples were drawn from the femoral arterial catheter. 200 μL of blood was taken at zero time and the infusion started. Thereafter, 200 μL of blood was taken in 20 minute intervals for 1.5 hours. After each sampling, the arterial catheter was flushed with heparinized saline (100 U/mL).

Table 4.1. Initial weights and specific growth rates (over final four days of experiment) of rats fed folate-deficient or folate-replete Dyets Inc. amino acid-defined diet (#517777 and #517802 respectively). Values are given as: mean (S.D.) and n=6. There were no significant differences between the folate-replete and folate-deficient group (p <0.05) on the basis of a two-tailed t-test.

	Folate-Replete	Folate-Deficient
Initial Weight (g)	67 (4.1)	65 (4.4)
SGR (g gained •d^{-1} •g body wieght^{-1})	0.035 (0.0078)	0.032 (0.0078)
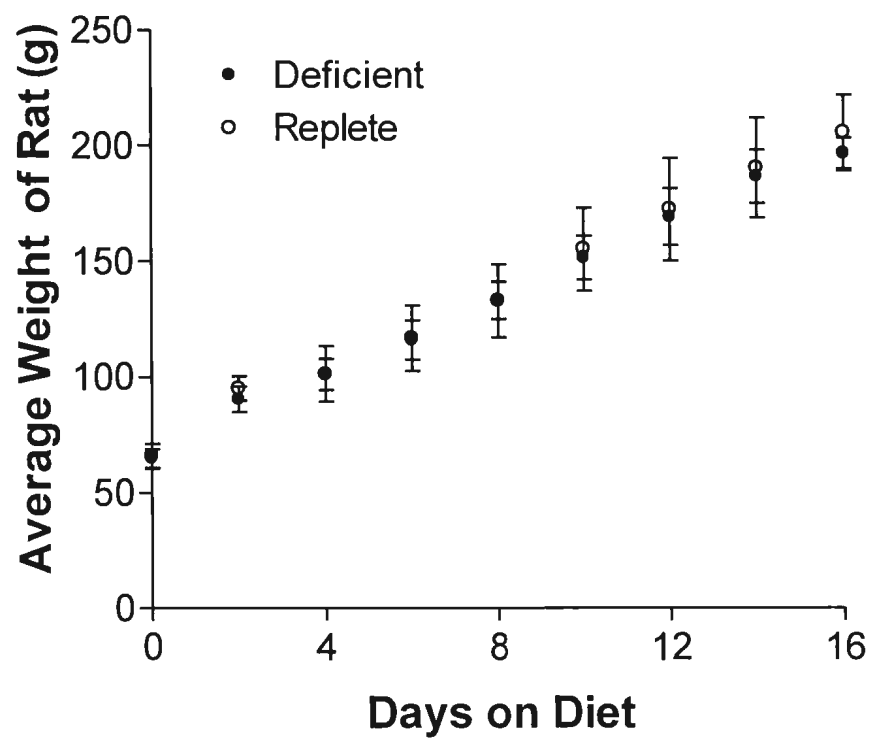
Figure 4.1. Average weights of rats fed either the folate-replete (cat. #517802) or folate-deficient (cat. #517777) version of of the Dyets Inc. amino acid-defined diet for 15 days. Error bars indicate standard deviation for the weight of rats and n=6.

4.4 Results

Rats undergoing a constant infusion of sodium ^{13}C-formate reached a steady-state plateau of isotopic enrichment within one hour (e.g. Figure 4.2 and 4.3). There were no obvious differences between the groups in the time needed to reach a plateau. This resulted in a TTR of ~6% for rats fed a folate-replete diet (Dyets cat. #517808), and ~10% in rats given a folate-deficient diet (Dyets cat. #517777) (Table 4.2). This corresponds to an endogenous formate production rate of 75 μmol/hr/100 g in folate-replete rats, with folate-deficient rats at about half this rate at 45 μmol/hr/100 g (Figure 4.4).

Endogenous formate production can be compared to the total dietary intake of potential formate precursors by measuring daily food intake and using knowledge of catabolic pathways capable of yielding formate and one carbon-bearing folates (Table 4.3). We found that endogenous formate production accounted for 35% of total ingested 1C precursor potential in folate-replete animals, and 20% in folate-deficient animals (Figure 4.5). However, this estimate assumes that all of the dietary amino acids are available for catabolism. This is not so as our rats continued to grow. We estimated amino acid utilization for net protein synthesis from knowledge of the protein content of the whole male Sprague-Dawley rat (*54*), the amino acid profile of whole rat protein (*55*) and the specific growth rate of rats over the final four days of the experiment.

These rats will lay down 6g of new tissue in 24 hours, of which 1.194 g will be protein. We therefore calculated the quantity of each of methionine, glycine, serine, histidine and tryptophan that will be incorporated into net protein. This was subtracted from the quantity of each amino acid ingested to provide a more accurate estimate of the quantity of each amino acid available for formate production.
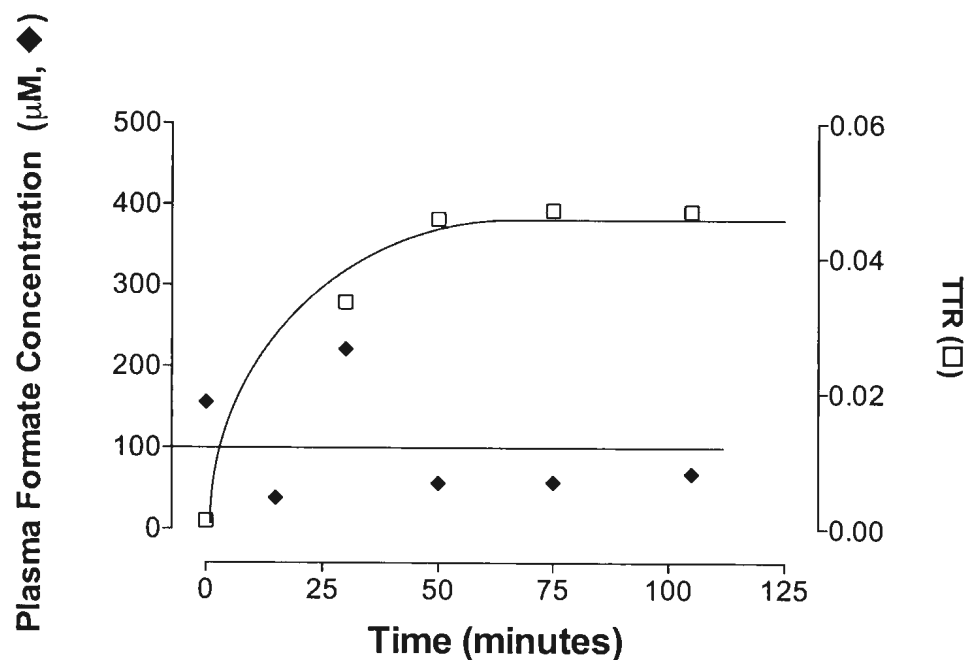
Figure 4.2. Typical timecourse for plasma formate concentration and TTR over ~2

hours for a rat undergoing a constant infusion of sodium ^{13}C-formate (8.8 μmol/hr).

The plasma concentration remains constant, and isotopic equilibrium is reached

after one hour. This particular rat was fed a folate-replete version of the Dyets Inc.

amino acid-defined diet (cat. #517802) for 15 days.
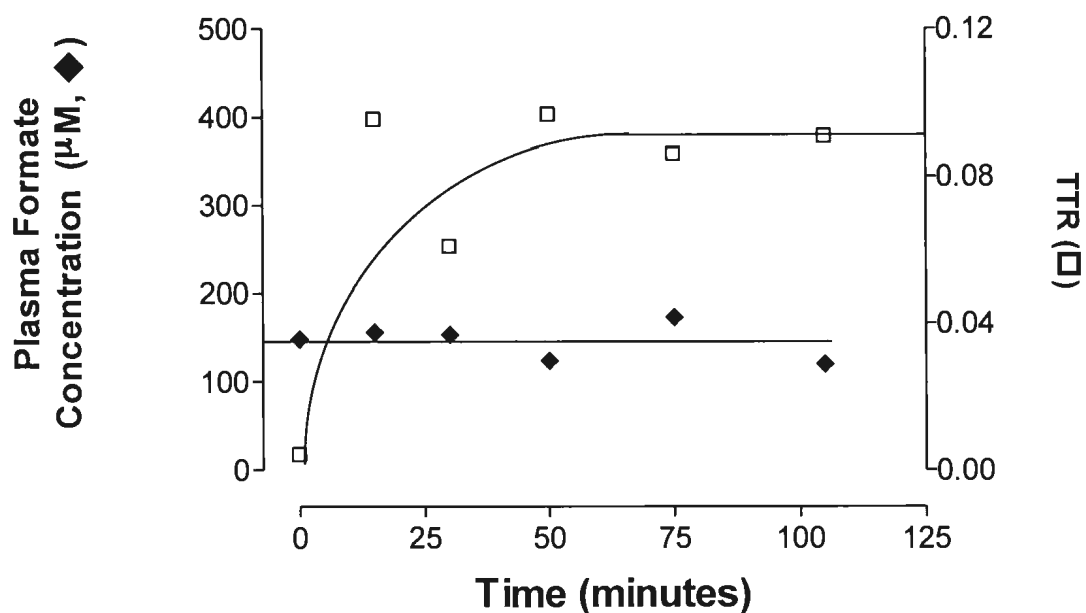
Figure 4.3. Typical timecourse for plasma formate concentration and TTR over ~2 hours for a rat undergoing a constant infusion of sodium ^{13}C-formate (8.8 μmol/hr). The plasma concentration remains constant, and isotopic equilibrium is reached after one hour. This particular rat was fed a folate-deficient version of the Dyets Inc. amino acid-defined diet (cat. #517777) for 15 days.

Table 4.2. TTR (^{13}C-formate to ^{12}C-formate), plasma formate concentration and rate of endogenous formate production (per 100g rat body weight) compared between folate-replete and folate-deficient rats having undergone a constant infusion of sodium ^{13}C-formate (8.8 μmol/hr) after attaining isotopic equilibrium. Values given as: mean (S.D) for each group of rats and n=6. Different superscripts indicate a signficant difference (P≤0.05) by two-tailed test, except for plasma formate concentration by one-tailed t-test.

	Plateau TTR	Plasma formate concentration (μM)	Rate of endogenous formate production (μmol/hr/100g)
Folate-Replete	0.0573 (0.0169)[a]	71 (28)[a]	76.2 (15.8)[a]
Folate-Deficient	0.0986 (0.0121)[b]	271 (119)[b]	43.5 (4.0)[b]
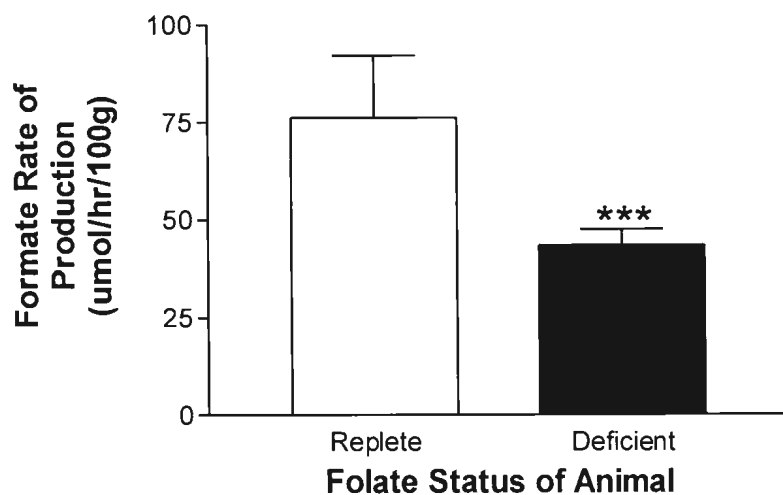
Figure 4.4. Comparison of rates of endogenous formate production between animals fed either a folate-deficient (Dyets Inc. #517777) or folate-replete (Dyets Inc. #517802) diet for 15 days. Bars indicate the average of the groups; error bars are standard deviation (n=6). Statistics by two-tailed t-test. Three asterisks indicate P≤0.001 by two-tailed t-test.

Table 4.3. Total 1C potential from average daily consumption (23 g for a 200g rat) of Dyets Inc. amino acid-defined diet. This is based on quantities of the 1C precursors consumed (column 3), and number of one-carbon groups, which can be maximally provided by each molecule during catabolism (column 4).

1	2	3	4	5	6
Precursor	g/kg diet	mmols/kg diet	Multiplier	1C Potential/kg diet (mmol)	1C Potential based on daily diet intake (mmol)*
Histidine	3.3	21.3	1	21.3	0.49
Tryptophan	1.74	8.5	1	8.5	0.20
Methionine	8.2	55.0	1	55.0	1.26
Glycine	23.3	310.4	1	310.4	7.14
Serine	3.5	33.3	2	66.6	1.53
Choline Chloride	2	14.4	4	57.6	1.32
Potential 1C Precursors in 1 KG diet (mmol)				519.3	
Potential 1C Precursors – average daily food intake (mmol)					11.963

*There was no difference between the food intake of the folate-replete and folate-deficient rats, so that our estimate of dietary 1C group potential is identical for both groups.
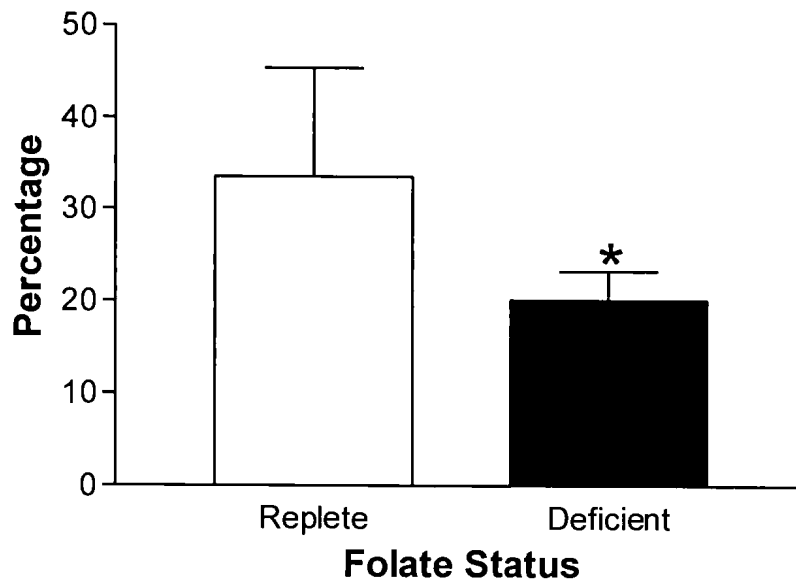
Figure 4.5. Actual endogenous formate production compared to ingestion of potential formate precursors. Animals were fed either a folate-deficient (Dyets Inc. #517777) or folate-replete (Dyets Inc. #517802) diet for 15 days, then given a constant infusion of sodium ^{13}C-formate (8.8 μmol/hr). Bars indicate the average of the group, error bars are standard deviation (n=6). One asterisk indicates P≤0.05 by two-tailed t-test.

We calculated that formate production amounts to 44% of the maximal possible one-carbon units available from the diet (subtracting that used for protein synthesis) in the folate-replete rats and 24% in the folate deficient rats (Table 4.4).

Figure 4.6 compares the plasma formate concentration to the hourly rate of formate production in folate-replete and folate-deficient animals. There is a remarkable differentiation between the responses of the two groups of animals. There was a positive relationship between both parameters in the folate-replete animals. However, in the folate-deficient animals, the highest levels of formate were accompanied by reduced rates of endogenous formate production.

4.5 Analysis

The positive correlation between formate concentration and formate production rates suggests that in this situation, the plasma formate concentration is largely determined by the rate of formate production. In folate-deficient rats, the opposite is found; a higher plasma formate concentration is associated with a lower rate of endogenous formate production. This inverse relationship leads us to conclude that folate-deficient rats have a significant decrease in both the production and removal of free formate.

The comparison of actual endogenous formate production to the ingested potential 1C precursors leads us to conclude that formate production may be a major, though ignored, motif for some of the dietary 1C precursors. After accounting for the amino acids required for net protein synthesis, we find that formate production accounts for nearly half of the available 1C precursor in the folate-replete rat, and close to a quarter in the folate-deficient rat.

Table 4.4. Estimation of quantity of known individual formate precursors that are required for net protein synthesis.

Amino Acid	Molar proportion of rat whole body protein (54)	Quantity of amino acid used for net protein synthesis (mmol/24h/200g rat)	Quantity of amino acid or choline provided in diet (mmol/24h/200g rat)	Quantity of amino acid or choline not used for net protein synthesis (mmol/24h/200g rat)
Histidine	0.0168	0.195	0.489	0.294
Trytophan	0.0140	0.161	0.196	0.035
Methionine	0.0220	0.253	1.264	1.011
Glycine	0.1611	1.853	7.139	5.286
Serine	0.0523	0.605	1.532	0.927
Choline	-	-	1.324	1.324
Total 1C potential based on remaining precursors once net protein synthesis accounted for (mmol)				8.88
Average endogenous formate production (24h) – in 200g folate-replete rat (mmol)				3.94
Actual endogenous formate production compared to available ingested 1C precursors, after accounting for new protein synthesis – in 200g folate-replete rat				44.4%
Average endogenous formate production (24h) – in 200g folate-deficient rat (mmol)				2.17
Actual endogenous formate production compared to available ingested 1C precursors, after accounting for net protein synthesis – in 200g folate-deficient rat				24.4%
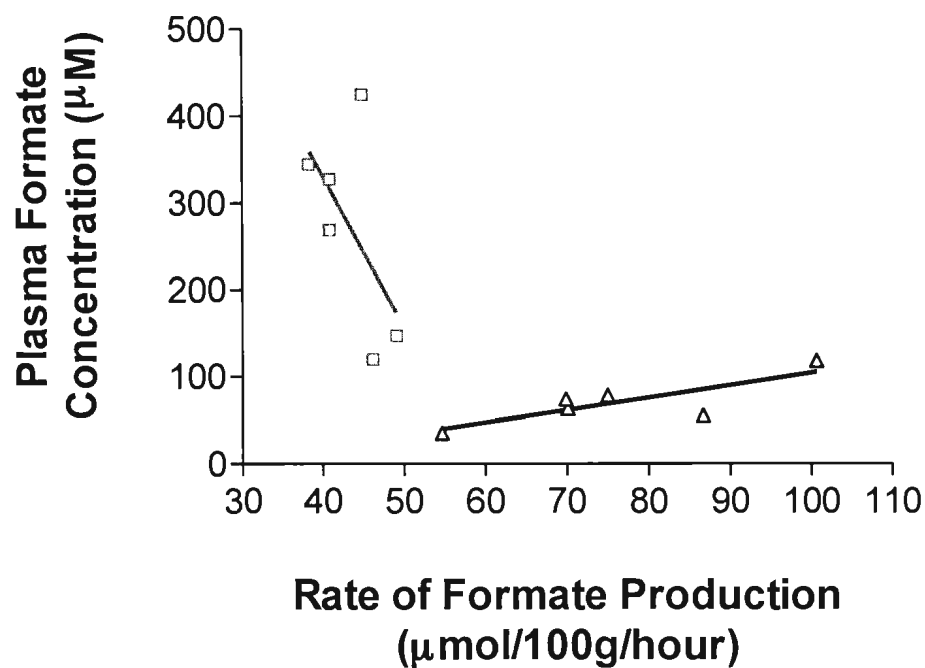
Figure 4.6. Comparison of the relationship between plasma formate concentra

the hourly rate of formate production rats fed either a folate-deficient (□) or fo

replete (Δ) diet for 15 days (n=6). Each point represents a single animal. The li

were fitted by least squares regression.

Chapter Five – Supplementation studies with dietary 1C precursors of the formate pool

5.1 One-carbon precursor supplementation I

5.1.1 Introduction

The first supplementation experiment with dietary one-carbon precursors was based on the idea that in those animals with elevated urinary formate excretion and plasma formate concentrations, the elevated formate must arise as a result of increased formate production from established one-carbon precursors. These precursors were discussed in the introduction, and are mainly derived from the catabolism of certain amino acids and choline. Equal numbers of rats were fed either a folate-replete or folate-deficient diet, based on the purified diet provided by Dyets Inc. (cat. #517802 and #517777 respectively). This trial ran for 15 days, with specific 1C precursor-supplemented diets being provided on the final 3 days (see details of diet modification in Appendix D). Animals were obtained in cohorts of fifteen, as they became available from the breeding stock. The initial weights, and specific growth rates (over the final four days) of rats fed each diet are provided in Table 5.1. Growth curves for rats fed the unsupplemented versions of the folate-replete and folate-deficient versions of the Dyets Inc. composition during this experiment are provided in Figure 5.1.

A distinguishing feature of this diet is that the protein content is derived from individual L-amino acids, allowing for a highly accurate measurement of the intake of each precursor. Precursors of interest included the amino acids tryptophan, glycine, serine, methionine and histidine. The non-amino acid choline and two of its metabolites DMG and sarcosine were also investigated.

Table 5.1. Initial weights and specific growth rates (for final four days) of rats fed control versions of the folate-replete and folate-deficient Dyets Inc. L-amino acid-defined diet (#517802 and #517777 respectively). Values are given as: mean (S.D.) for each group of rats and n=6. Different superscripts indicate that a significant difference exists between the folate-replete and folate-deficient groups (p <0.05) on the basis of a two-tailed t-test.

	Folate-Replete	Folate-Deficient
Initial Weight (g)	70.5 (9.2)	70.0 (8.2)
SGR (g gained •d^{-1} •g body wieght^{-1})	0.051 (0.0065)[a]	0.046 (0.0076)[b]
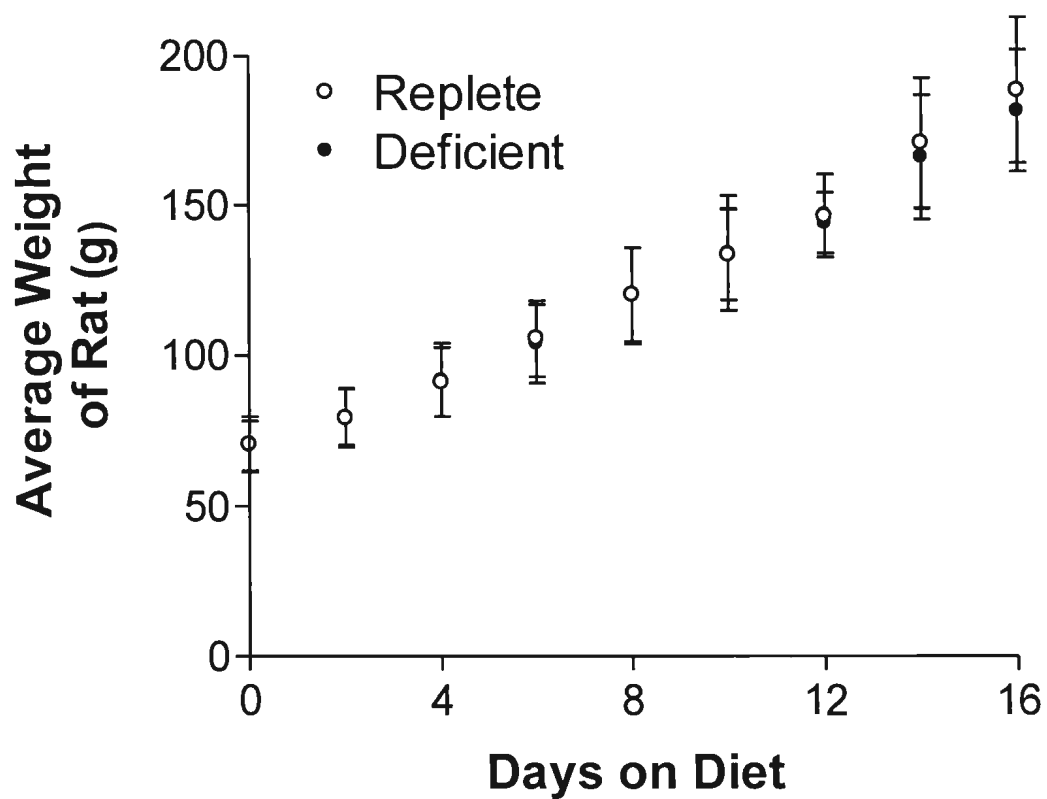
Figure 5.1. Average weights of rats fed either the folate-replete (cat. #517802) or folate-deficient (cat. #517777) version of of the Dyets Inc. L-amino acid-defined diet over the course of 15 days. Error bars indicate standard deviation of rat weights and n=6.

For supplemented experimental groups, we doubled the baseline diet concentration of the precursor of interest. Glycine was present in the highest quantity and so was simply doubled. All supplementations were isonitrogenous. As such, for 1C precursors present in lesser quantities, the molar difference was made up by extra alanine.

In order to ensure that the extra alanine did not affect results, an all-alanine supplementation group was also run. Due to the fact that the Dyets Inc. diet is pre-mixed, the mass of the whole diet was reduced according to the combined mass of 1C precursor and alanine added. These additions accounted for less than 1% of the overall mass, and as such all other components were reduced by this amount.

We staggered each supplementation group over several cohorts. The folate-replete/folate-deficient versions of the diet were staggered in the same way. In addition, we ran an early group of unsupplemented controls as well as a later group of unsupplemented controls, at both the folate-replete and folate-deficient levels in order to ensure comparability . These early and late unsupplemented controls were compared (using a separate t-test at each folate level). We used a one-way ANOVA to compare the folate-replete animals and another one-way ANOVA to compare the folate-deficient animals. Each 1C precursor supplementation group was compared to its respective control. In effect, this meant that the folate-deficient analysis was separate from the folate-replete analysis. With the exception of the unsupplemented controls (n=6), all experimental groups were run at a sample size of n=3. Since catalase may

clear excess formate rapidly, we compared liver catalase activity between control

folate-replete and control folate-deficient rats.

5.1.2 Results

The plasma formate concentration of rats fed a folate-replete version of the

Dyets Inc. L-amino acid-defined diet (#517802) supplemented with a variety of dietary

1C precursors is provided in Figure 5.2. Relative to the unsupplemented folate-replete

control group, extra glycine, histidine, serine, and tryptophan all increased the plasma

formate concentration significantly. Figure 5.3 provides similar information for

animals fed the supplemented Dyets Inc. folate-deficient diet (#517777). In this case

there was no significant difference between the formate levels of the different groups.

This may be due to high variability. It is worth noting that, although only two glycine-

supplemented folate-deficient rat plasma samples were successfully obtained, the

mean is nearly half that of the unsupplemented folate-deficient control.

Figures 5.4 and 5.5 show the 24 hour excretion of urinary formate, normalized

to creatinine excretion, for rats fed either the folate-replete or deficient diets and

supplemented with dietary 1C precursors. Among the rats fed the folate-replete diet

only serine supplementation resulted in significantly elevated formate excretion, while

in the folate-deficient supplementations only DMG supplementation resulted in

significantly elevated formate excretion.

Catalase, an enzyme capable of large-scale catabolism of formate, was equally

active in rats fed either folate-deficient or folate-replete diets (Figure 5.6).
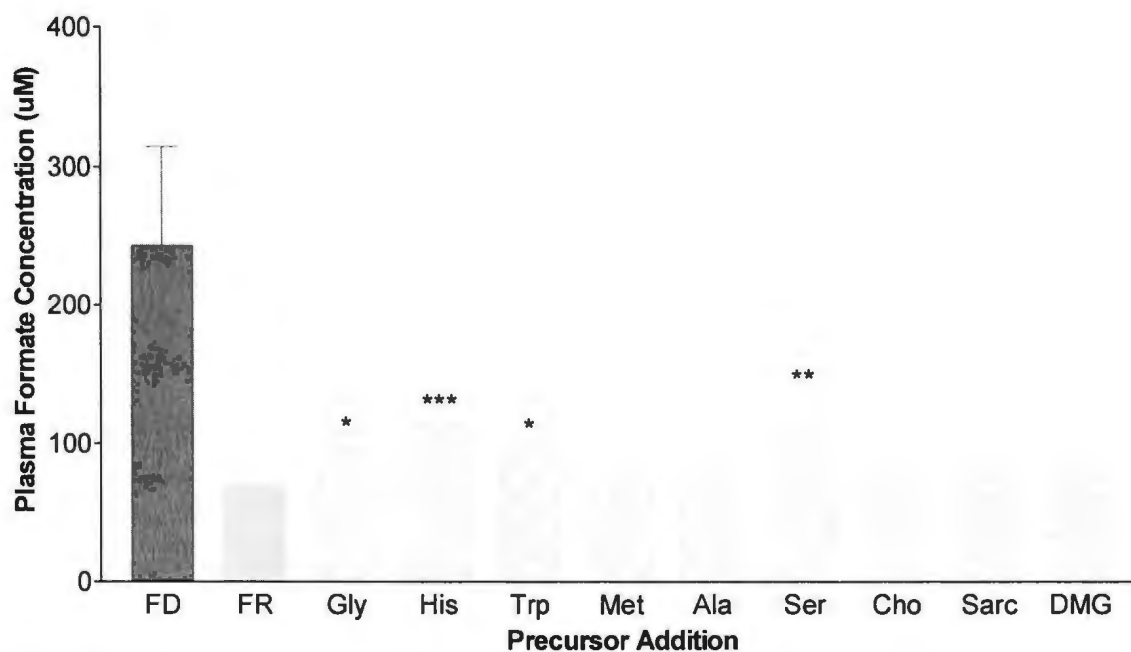
Figure 5.2. Plasma formate level for rats fed a folate-replete L-amino acid-defined diet (Dyets Inc. #517802) for 15 days, supplemented with extra one-carbon precursors for the final 3 days. Specific supplementations are described in Appendix D. Bars represent the mean of the group; error bars are standard deviation. The unsupplemented folate replete group (n=6) is solid green; supplemented groups are shaded green (n=3). The corresponding control for animals fed a folate-deficient diet is shown as solid red (n=6) to allow for comparison. Statistics were carried out by one-way ANOVA with comparisons against the folate-replete unsupplemented control and alanine groups (one asterisk indicates $P \leq 0.05$, two asterisks indicates $P \leq 0.01$, three asterisks indicates $P \leq 0.001$). Abbreviations: FD – unsupplemented folate-deficient, FR – unsupplemented folate-replete.
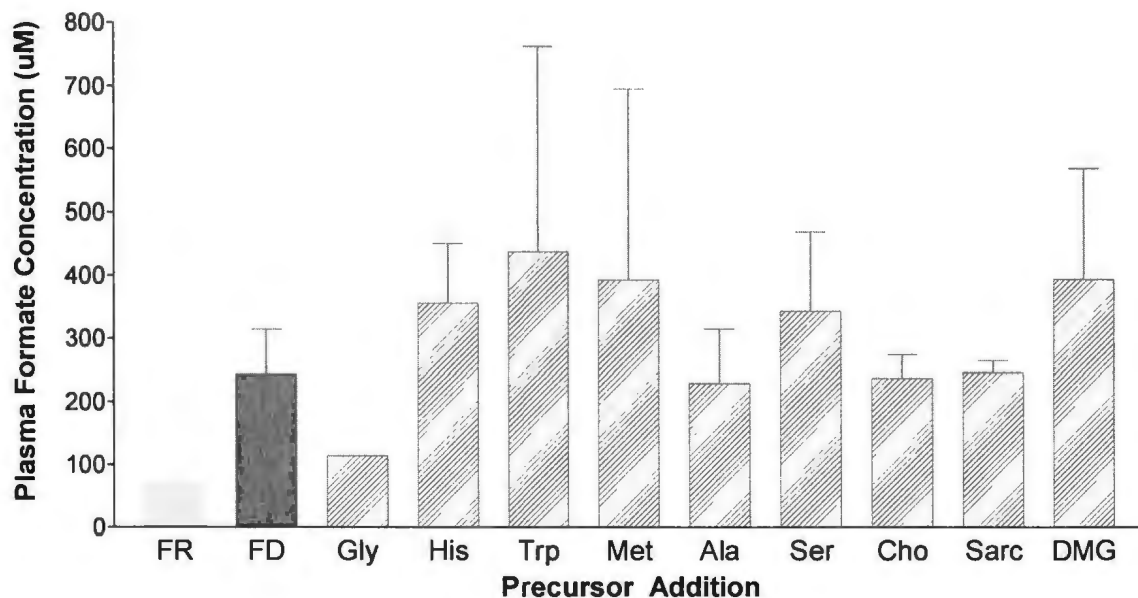
Figure 5.3. Plasma formate level for rats fed a folate-deficient L-amino acid-defined diet (Dyets Inc. #517777) for 15 days, supplemented with extra one-carbon precursors for the final 3 days. Specific supplementations are described in Appendix D. Bars represent the mean of the group; error bars are standard deviation. The unsupplemented folate-deficient group (n=6) is solid red; supplemented groups are shaded red (n=3, except glycine n=2). The corresponding control for animals fed a folate-replete diet is shown as solid green (n=6) to allow for comparison. Statistics were carried out by one-way ANOVA with comparisons against the folate-deficient control and alanine groups; no significant differences were found. Abbreviations: FD – unsupplemented folate-deficient, FR – unsupplemented folate-replete.
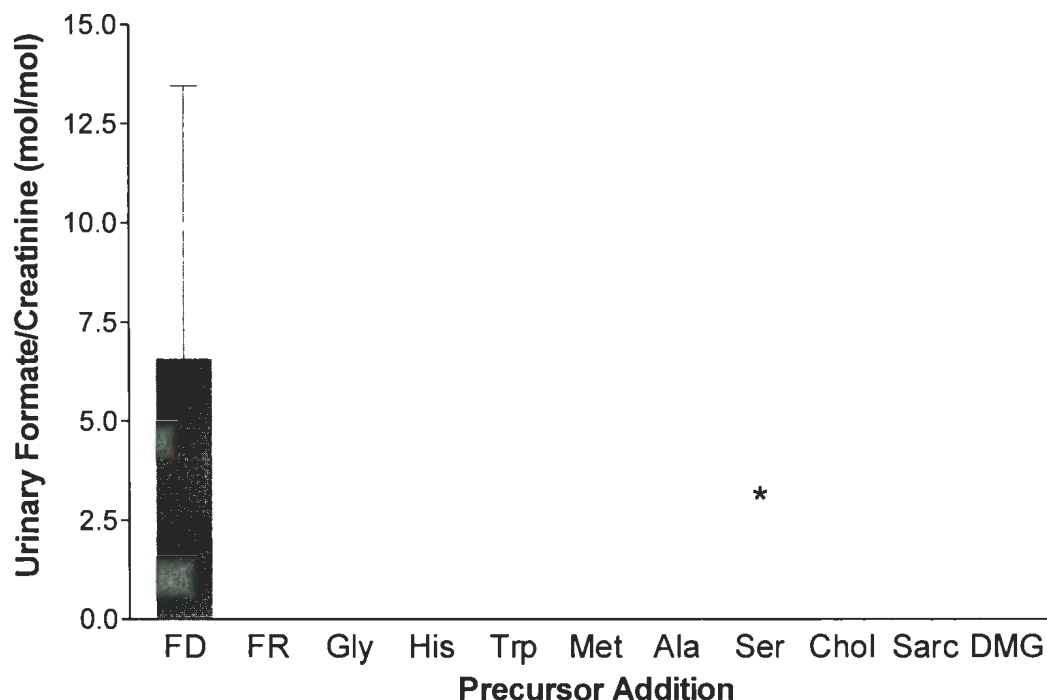
Figure 5.4. 24 hour formate excretion, normalized to creatinine excretion, in the urine of rats fed a folate-replete L-amino acid-defined diet (Dyets Inc. #517802) for 15 days, supplemented with extra one-carbon precursors for the final 3 days. Specific supplementations are described in Appendix D. Bars represent the mean of the group; error bars are standard deviation. The unsupplemented folate replete group (n=6) is solid green; supplemented groups are shaded green (n=3). The corresponding control for animals fed a folate-deficient diet is shown as solid red (n=6) to allow for comparison. Statistics were carried out by one-way ANOVA with comparisons against the folate-replete control and alanine groups (one asterisk indicates P≤0.05). Abbreviations: FD – unsupplemented folate-deficient, FR – unsupplemented folate-replete.

Figure 5.5. 24 hour formate excretion, normalized to creatinine excretion, in the urine of rats fed a folate-deficient L-amino acid-defined diet (Dyets Inc. #517777) for 15 days, supplemented with extra one-carbon precursors for the final 3 days. Specific supplementations are described in Appendix D.Bars represent the mean of the group; error bars are standard deviation. The unsupplemented folate-deficient group (n=6) is solid red; supplemented groups are shaded red (n=3). The corresponding control for animals fed a folate-replete diet is shown as solid green (n=6) to allow for comparison. Statistics were carried out by one-way ANOVA with comparisons against the folate-replete control and alanine groups (one asterisk indicates $P \leq 0.05$). Abbreviations: FD – unsupplemented folate-deficient, FR – unsupplemented folate-replete.
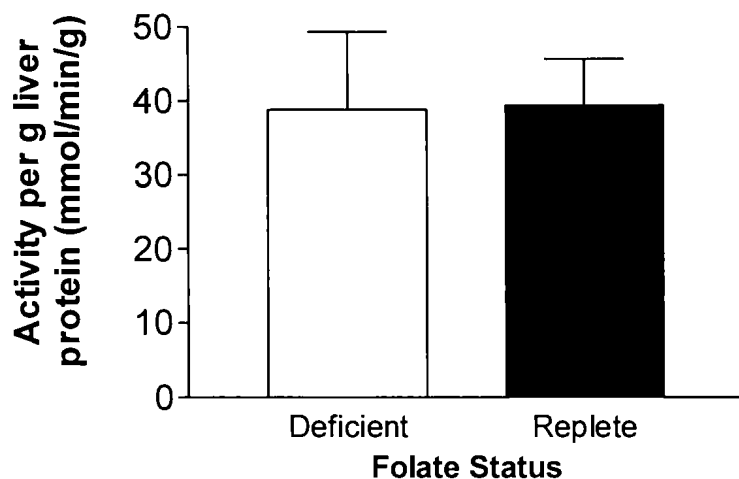
Figure 5.6. Catalase activity in the livers of rats fed either a folate-deficient Dyets (cat. #517777) or folate-replete Dyets(cat. #517802) L-amino acid-defined diet for 15 days. Activity is defined as the mmoles of hydrogen peroxide converted to oxygen and water per minute per gram of liver protein. Bars represent the mean of each group, error bars are standard deviation. Means were compared using a two-tailed t-test.

5.2 Establishing another model for folate-deficiency in the rat.

5.2.1 Selecting a diet

The differences seen in both plasma formate levels and urinary formate excretion were in line with what we expected in folate-deficient rats compared to folate-replete rats(12). Despite this, we were concerned by the unusually high quantity of glycine present in the Dyets Inc. composition (as compared to the American Institute of Nutrition's recommendations for experimental rodent diets) due to its ability to generate 1C groups(41). We decided to compare the effect of casein-based AIN-93G diet against the amino acid-defined diet from Dyets Inc. in a side-by-side experiment.

Appendix B provides a comparison of the amino acid composition of the AIN-93G-based diet and the Dyets Inc. diet. The detailed compositions of both diets are provided in Appendix C. MP Biomedical offers a high-nitrogen casein which is purified in order to minimize vitamin content. This was used to create the AIN-93G-based diets. The opportunity arose to send the Dyets compositions to Dr. Mcfarlane (of Health Canada) for folate analysis of the folate-replete and folate-deficient versions, the results of which are also included in Appendix C. A microbiological assay was used because it is able to quantify all variants of folate/folic acid regardless of the length of glutamate tail or oxidation state.

We conducted a study to compare the two diets. Four diet groups were established with four rats in each group. The initial weights are provided in Table 5.2. The diet groups were Dyets folate-replete, Dyets folate-deficient, AIN-93G folate-replete, and AIN-93G folate-deficient. After 9 days, 2 animals from each subgroup were sacrificed and blood was collected and plasma prepared. After 18 days, the remaining 8 animals were

75

Table 5.2. Initial weights for rats fed either the folate-replete or folate-deficient form of a commercially produced amino acid-defined diet (Dyets Inc.), or on the AIN-93G-based diet. 4 rats began each of the 4 diets. Mean weights are given with standard deviations in parentheses. No significant differences were found using two-tailed t-tests.

	Dyets Inc.		AIN-93G	
Folate Status	Deficient	Replete	Deficient	Replete
Initial Weight (g)	68.3 (3.4) g	72.3 (5.30) g	71.8 (7.8) g	70.5 (6.7) g

sacrificed, and blood was sampled and plasma collected. Plasma homocysteine and formate were measured in order to establish folate-deficiency in each group. Statistics were not determined the sample size was too small (n=2). Figure 5.7 provides the growth curves for rats fed each of the four diets over the course of 18 days, which show that by the end of the 18 day trial, the rats fed an AIN-93G-based diet weighed slightly more than those rats fed the Dyets Inc. diet.

A comparison of the plasma formate concentrations between rats fed either a Dyets Inc. or AIN-93G-based diet showed that neither diet induced an appreciable level of folate-deficiency after 9 days (Figure 5.8). Both diets (in both the folate- replete and folate-deficient forms) resulted in a plasma formate concentration of ~50 µM. After 18 days, the folate-replete animals showed similar formate levels as those recorded at 9 days; however the plasma formate concentrations of animals fed the folate-deficient versions of either diet nearly tripled. We concluded that neither diet has a clear advantage in inducing folate-deficiency based on these data.

Figure 5.9 shows that after 9 days, the folate-deficient version of both diets resulted in a plasma homocysteine concentration twice that of the respective folate-replete diets. After 18 days, the AIN-93G-based diet produced a two-fold increase in plasma homocysteine concentration over the control diet. By comparison, the Dyets (#517777) folate-deficient diet produced a six-fold increase in plasma homocysteine over the control diet (#517802) at 18 days.

The preceding results indicate that both diets could have been used to induce a moderate folate-deficiency within similar periods of time. AIN-93G did provide two

77
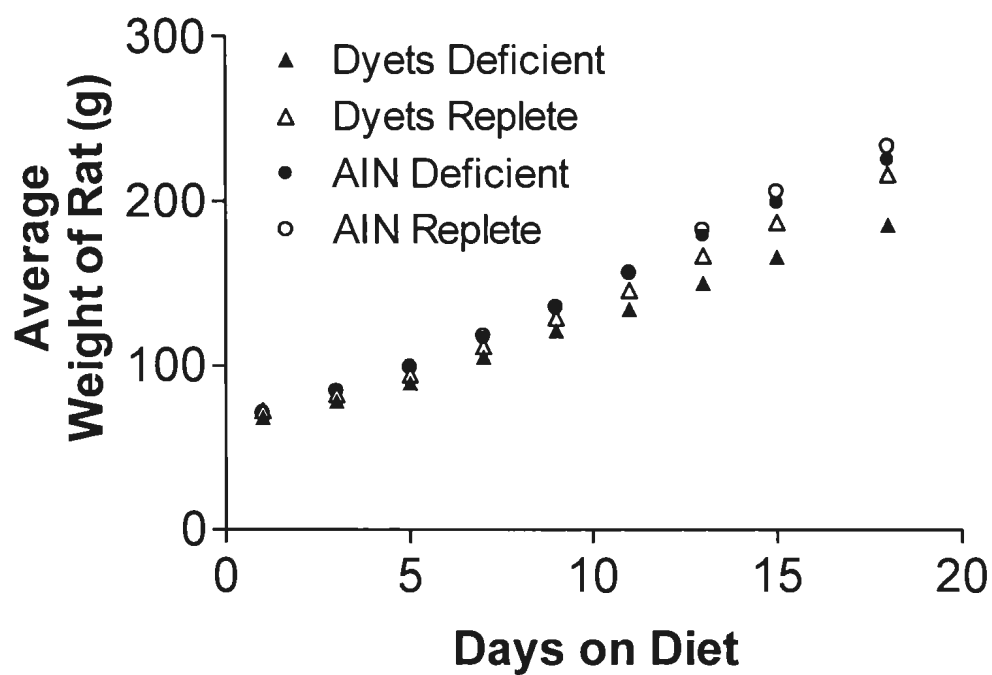
Figure 5.7. Average weights of rats fed either a folate-replete or folate-deficient version of either an AIN-93G-based diet or amino acid-defined diet produced by Dyets Inc. (cat. #517777 - folate-deficient, Cat. #517802 – folate-replete) for up to 18 days. The data are the average of two animals per category.
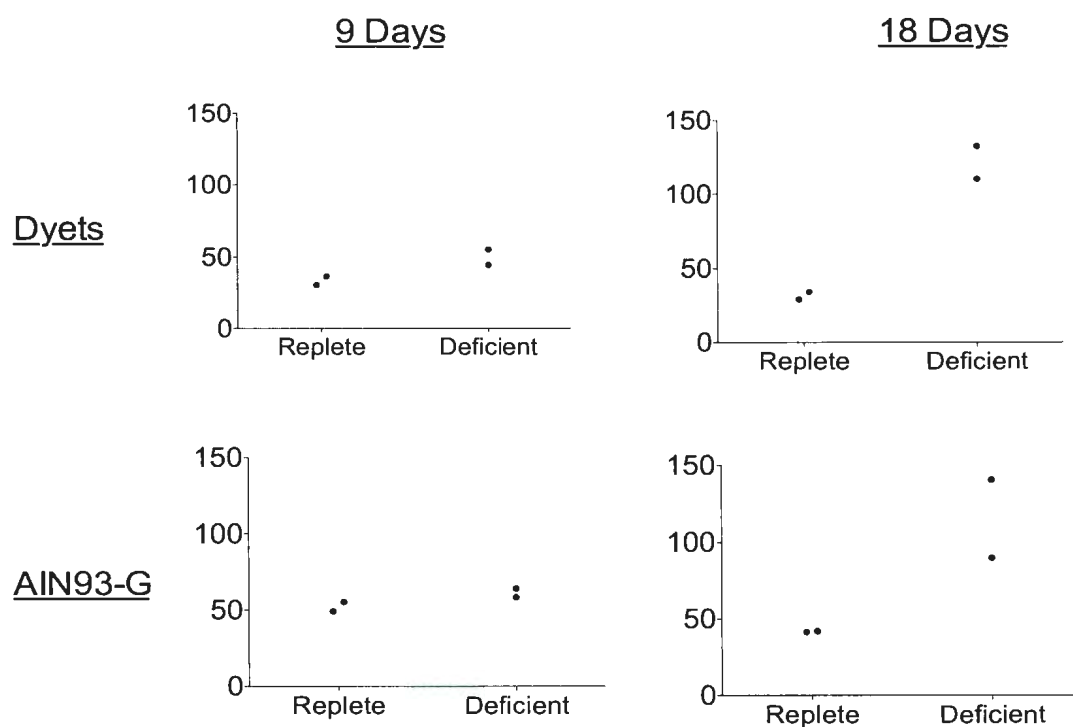
Figure 5.8. Plasma formate concentration (y-axes; uM) of rats fed either an AIN-93G-based or amino acid-defined Dyets Inc. (Cat. #517777, 517802) diet for either 9 or 18 days (both normal and folate-deficient varieties of each were tested). The data are the averages of two animals per category.
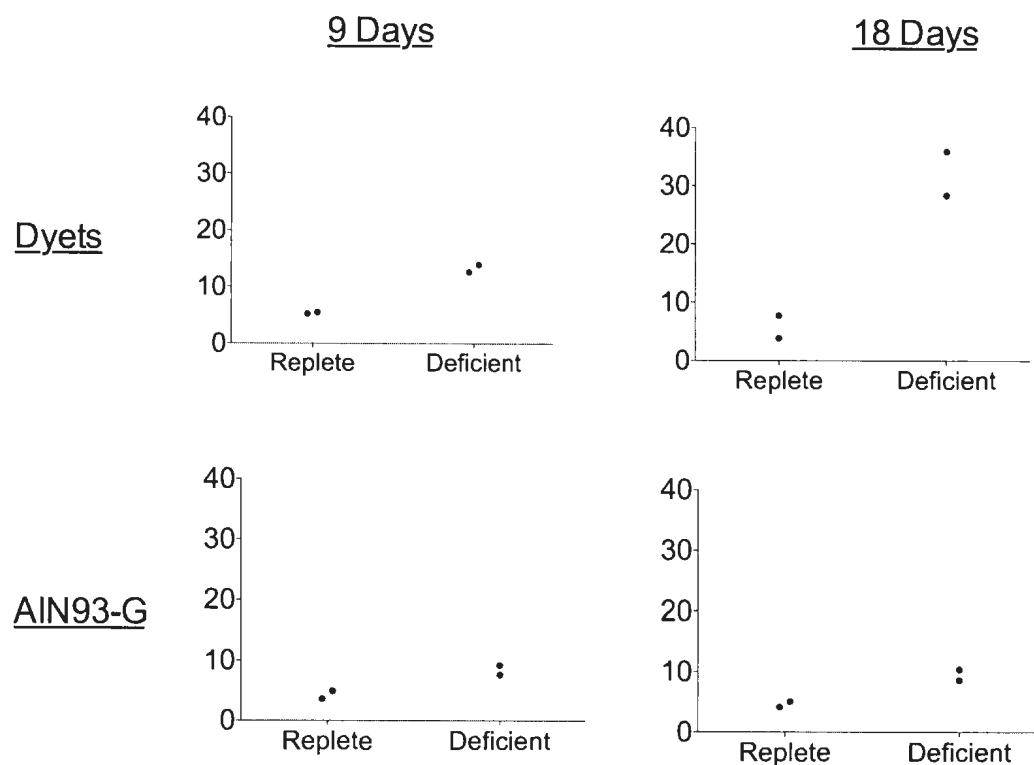
Figure 5.9. Plasma homocysteine concentration (y-axes; uM) of rats fed either an AIN-93G-based or amino acid-defined Dyets Inc. (Cat. #517777, 517802) diet for either 9 or 18 days (both normal and folate-deficient varieties of each were tested). The data are the averages of two animals per category.

key advantages compared to Dyets. One of our primary goals was to supplement the chosen diet with extra dietary 1C precursors, a process which would be simpler with a diet that we produce (AIN-93G). Since we prepare this diet from stock ingredients, we could increase or decrease specific components as necessary, an option not available with Dyets, because the composition arrives pre-mixed. Secondly, we were concerned by the high levels of glycine in the Dyets mixture (~20% of total amino acids by mass), a level that was several fold-higher than that recommended by the American Institute for Nutrition (*41*).

5.2.2 Establishing an experimental timescale

Following this comparison, we began studies on folate-deficiency using rats fed the AIN-93G-based diet. The initial objective was to determine the time course for induction of mild folate-deficiency. We set up a feeding study using AIN 93G diet (folate-replete and folate-deficient) for 30 days. At successive six day intervals, we sacrificed 6 rats (3 from each group) and measured the concentrations of formate and homocysteine in the plasma, as well as the daily excretion of formate in the urine.

Growth curves for both groups of rats are provided in Figure 5.10. Both the folate-replete and folate-deficient versions of the AIN-93G-based diets resulted in a consistent and comparable increase in weight.

Dietary folate status had no effect on plasma formate concentration after 6 days (see Figure 5.11). We saw some difference in plasma formate concentration between groups after 12 days and 24 days, although there was large within-group variance. Plasma formate concentration was significantly different at 18 days and 30 days.
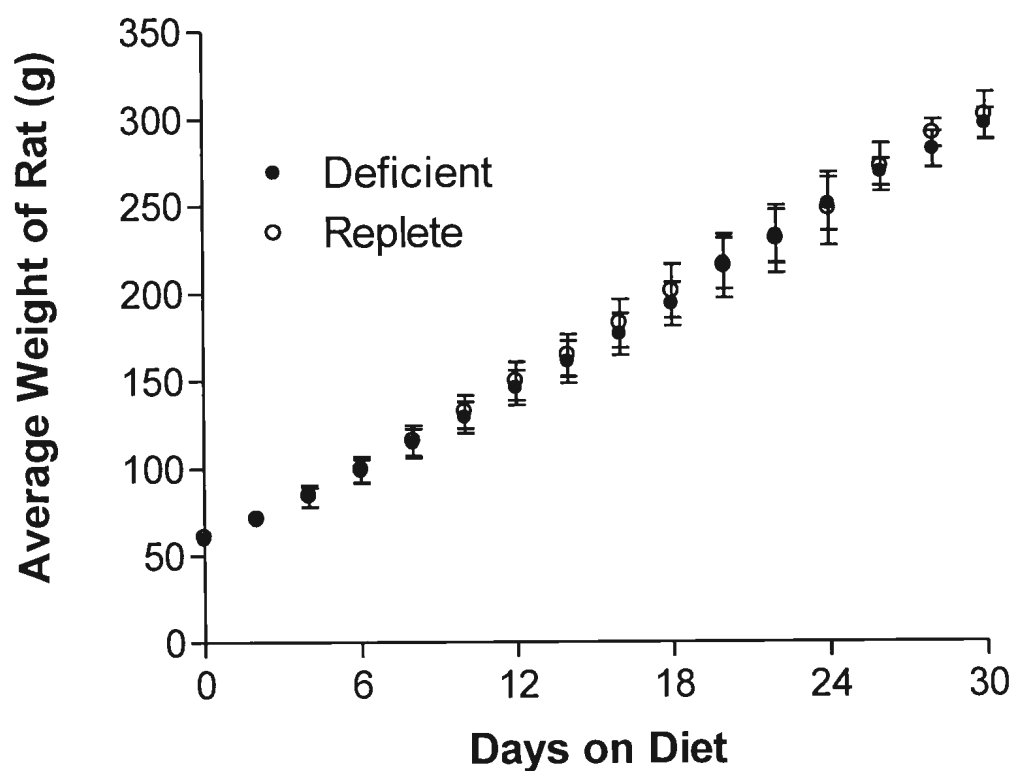
Figure 5.10. Average weights of rats fed either the folate-replete or folate-deficient AIN-93G-based diet for up to 30 days. Sample size decreases with increasing time(days 0-12; n=12, days 14-18; n=9, days 20-24; n=6, days 26-30; n=3). Error bars indicate standard deviation.
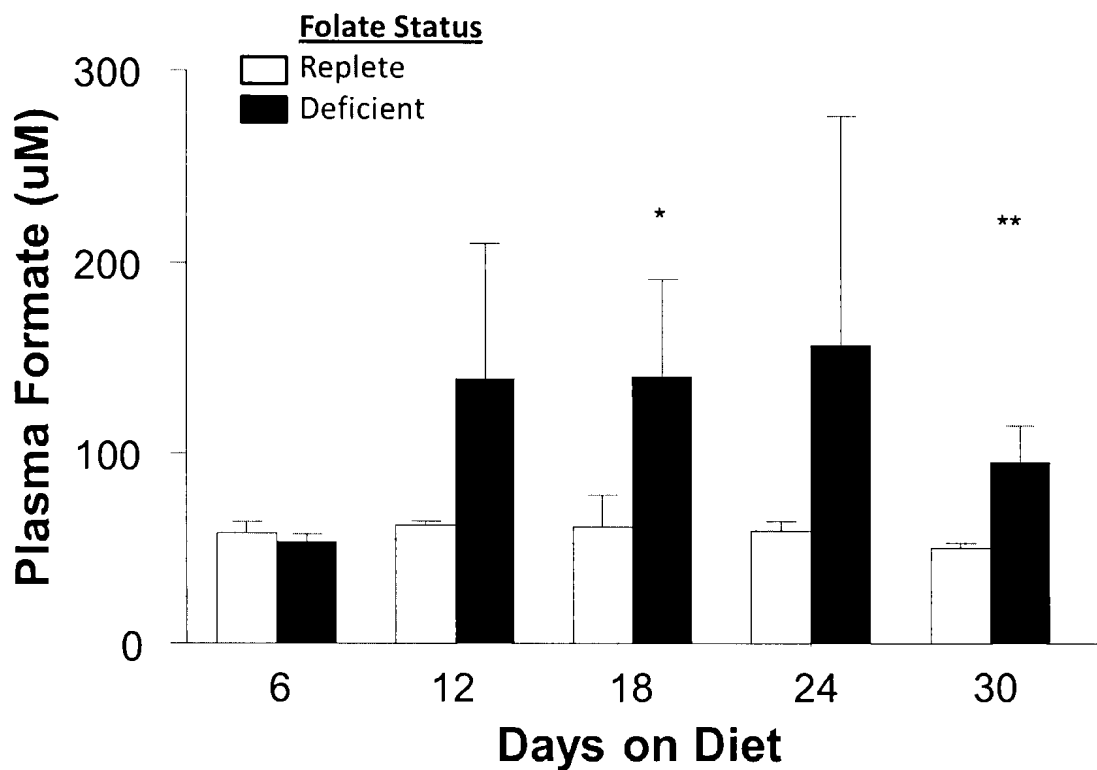
Figure 5.11. Plasma formate levels in rats fed an AIN-93G-based diet with and without folic acid for up to 30 days (n=3). Bars represent the mean of each group, error bars are standard deviation. One asterisk indicates statistical significance of $P \leq 0.05$, two asterisks indicates $P \leq 0.01$ by one-tailed t- test. Each test for significance compares the folate-deficient rats against a group of rats fed a folate-replete diet for the same number of days.

Plasma homocysteine was not affected by folate status until 18 days of feeding (Figure 5.12), when the concentration in folate-deficient rats increased to twice that of the folate-replete rats. Homocysteine remained elevated after 24 or 30 days, although the within-group variance becomes larger.

24 hour formate excretion in the urine is shown in Figure 5.13. Although formate excretion in folate-deficient animals appears to begin to exceed that of the corresponding folate-replete rats after 12 days, the only comparison where significance is achieved is at 18 days.

One-tailed t-tests were used in each of the above analyses, as it had already been established that under conditions of folate-deficiency, elevations above baseline would be observed in plasma formate, urinary formate excretion and plasma homocysteine (*12*).

Minimizing variance within an experimental treatment (small standard deviation) is important due to the fact that it allows for smaller experimental groups and consequently less animal usage. We would naturally choose the shortest viable timescale in order to economize our resources. Considering these points and the data, we selected 18 days as the ideal length of time to induce mild folate deficiency in rats fed an AIN-93G-based diet.
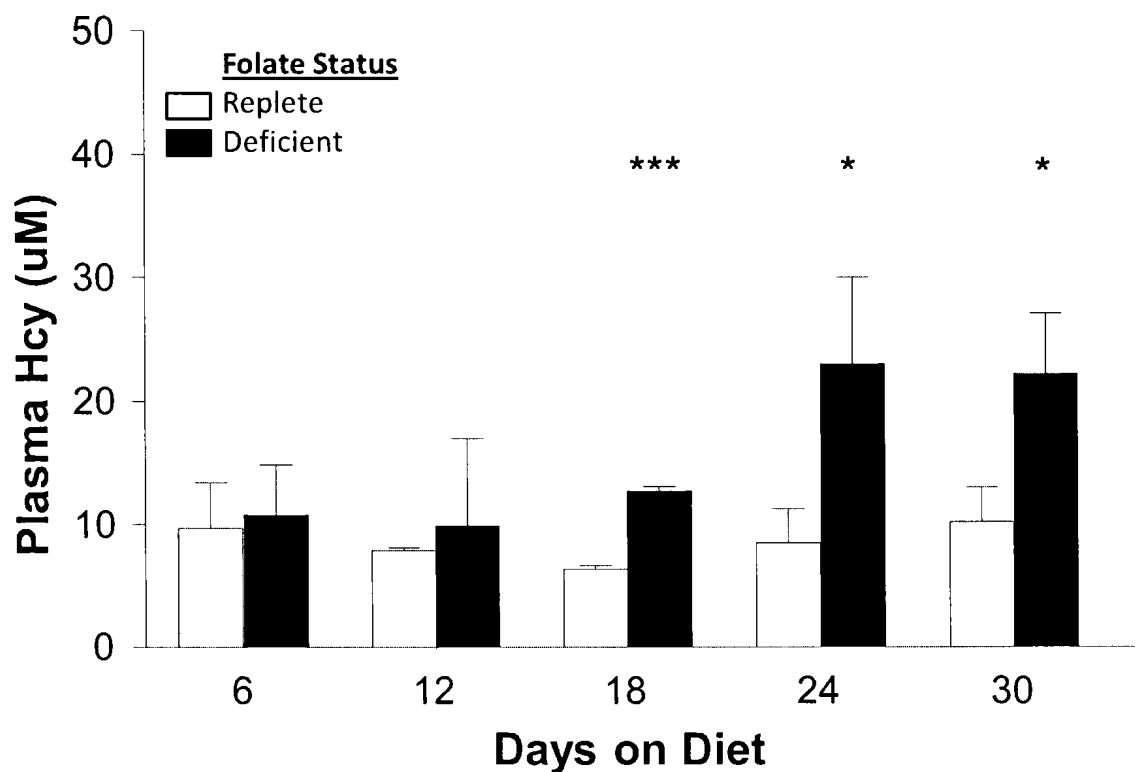
Figure 5.12. Plasma homocysteine levels in rats fed an AIN-93G-based diet with and without folic acid for up to 30 days (n=3). Bars represent the mean of each group, error bars are standard deviation. One asterisk indicates statistical significance of $P \leq 0.05$, three asterisks indicates a significance of $P \leq 0.001$ by one-tailed t- test. Each test for significance compares the folate-deficient rats against a group of rats fed a folate-replete diet for the same number of days.
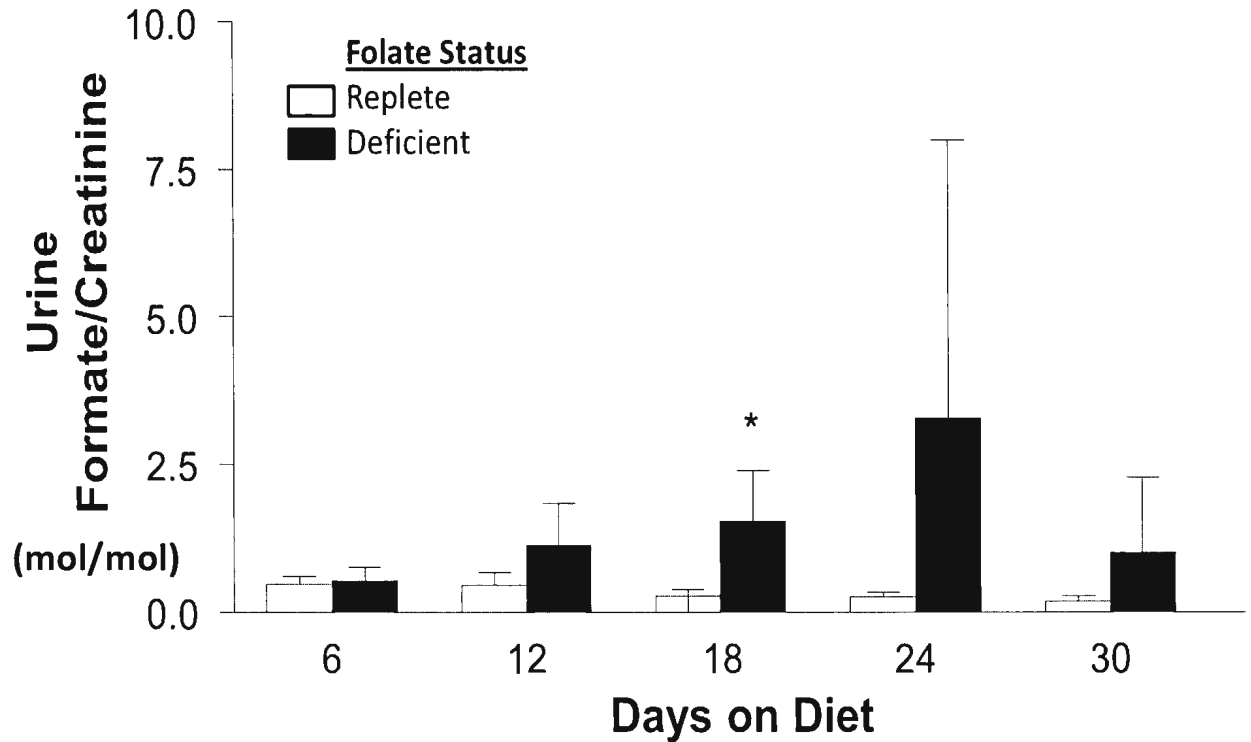
Figure 5.13. 24 hour formate excretion in urine, normalized to creatinine excretion, for rats fed an AIN-93G-based diet with and without folic acid for up to 30 days (n=3). Bars represent the mean of each group, error bars are standard deviation. One asterisk indicates statistical significance of $P \leq 0.05$ by one-tailed t- test. Each test for significance compares the folate-deficient rats against a group of rats fed a folate-replete diet for the same number of days.

5.3 One-carbon precursor supplementation II

5.3.1 Objectives

A second one-carbon precursor supplementation experiment was carried out in which a number of modifications were made. The principal difference was that a casein-based diet (AIN-93G) was employed in place of the Dyets Inc. diet. The animals were fed for 18 days, and were placed on individual one-carbon precursor supplemented diets for the final five days (rather than three). All dietary 1C precursors studied were increased by 46 mmol per kilogram of prepared diet. This amount of supplementation was chosen to provide a 50% increase in the dietary level of serine. A corresponding mass reduction in corn starch (the most abundant ingredient in the diet) offset this addition. Details of the composition of the AIN-93G-based diets are provided in Appendix C, and modifications resulting from 1C precursor supplementation to these diets are in Appendix E. We did not supplement with sarcosine or DMG since they are not provided in the diet, but rather are produced in the body through the catabolism of choline.

During the first 1C precursor supplementation study we found that there appeared to be greater variance in the plasma and urine formate concentrations in the folate-deficient rats. We addressed this by assigning a greater number of our available animals to the folate-deficient groups. 90 male Sprague-Dawley weanling rats arrived in 2 cohorts (A&B). Cohort A consisted of 50 animals, while Cohort B contained 40 animals. The distribution of cohorts, and supplemented diet assignments are provided in Table 5.3.

Table 5.3. Organization of the 18 day, one-carbon precursor supplementation study using AIN-93G-based diet (carried out using two cohorts of animals). For each supplementation group (or unsupplemented control), 6 rats were given a folate-deficient diet, and 4 rats received the corresponding folate-replete diet. Cohorts A and B are shown below. Both cohorts were combined to form the third table which represents the overall experimental design.

		Precursor Supplementation Cohort A (n=50)				
		Ctrl A	Serine	Tryptophan	Alanine	Glycine
Folate Status of Diet	Replete	4	4	4	4	4
	Deficient	6	6	6	6	6

		Precursor Supplementation Cohort B (n=40)			
		Ctrl B	Histidine	Methionine	Choline
Folate Status of Diet	Replete	4	4	4	4
	Deficient	6	6	6	6

		Combined Cohorts (n=90)							
		Ctrl	Ala	Met	Gly	Ser	Trp	His	Choline
Folate Status of Diet	Replete	8	4	4	4	4	4	4	4
	Deficient	12	6	6	6	6	6	6	6

We also compared the plasma homocysteine levels of choline-supplemented animals with other one-carbon precursor supplemented rats as well as unsupplemented rats, within the folate-replete and folate-deficient groups. This analysis was of interest because betaine (a catabolite of choline), in concert with betaine: homocysteine methyltransferase, can remethylate homocysteine to produce methionine, effectively lowering the baseline homocysteine concentration.

The combined experimental design served as the basis of the statistical analysis for the plasma formate concentration and urinary formate excretion. During our planning stages, and in consultation with a statistician (Dr. David Schneider, Memorial University, Canada), we devised a series of a priori comparisons, in which each supplementation group was compared against its appropriate unsupplemented control (either at the folate-replete or folate-deficient level). For the purposes of this analysis, we treated the alanine supplementation group as part of the unsupplemented control on the grounds that it lacks any additional one-carbon potential. T-tests were used to determine that it did not differ from the unsupplemented controls of either the folate-replete or folate-deficient groups. The initial weights, and specific growth rates (over final four days) of rats fed each diet are provided in Table 5.4. Growth curves for rats fed the unsupplemented versions of the folate-replete and folate-deficient versions of the AIN-93G-based diet during this experiment are provided in Figure 5.14.

Table 5.4. Initial weights and specific growth rates (SGR) (over last four days of the experiments) of rats fed unsupplemented versions of the folate-deficient (n=12)and folate-replete (n=8) AIN 93G-based diet. Values are given as: mean (S.D.). Different superscripts indicate that a significant difference exists between the folate-deficient and folate-replete group ($p < 0.05$) on the basis of a two-tailed t-test.

	Folate-Replete	Folate-Deficient
Initial Weight (g)	62 (5.3)	58 (6.4)
SGR ($g\,d^{-1}\,g^{-1}$)	0.050 (0.0037)[a]	0.043 (0.0057)[b]
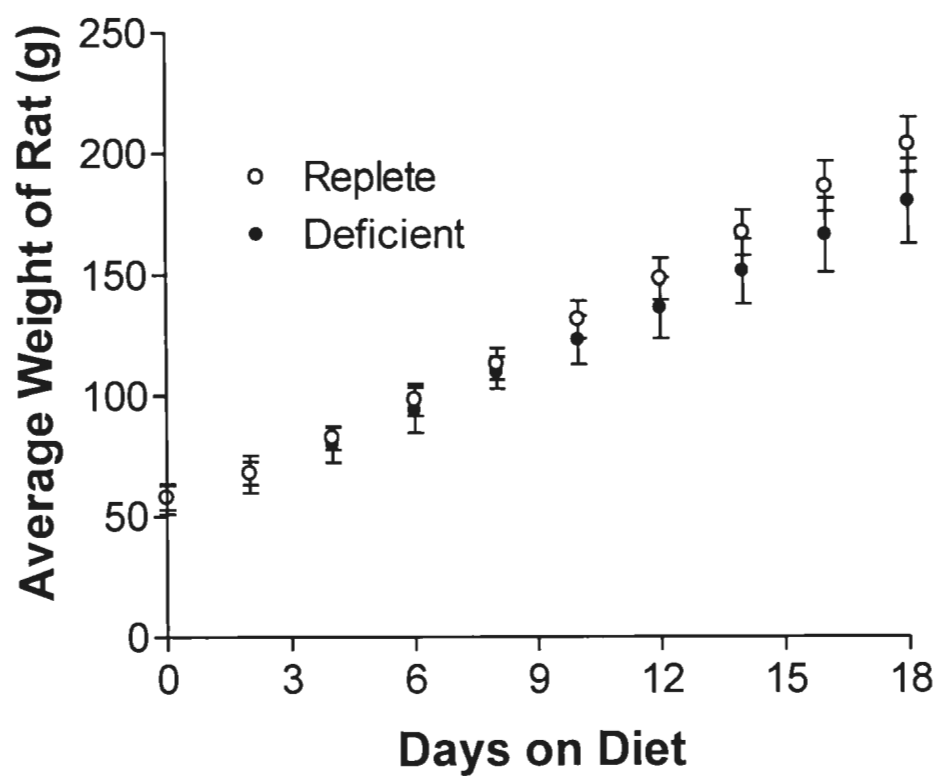
Figure 5.14. Average weights of rats fed either the folate-replete (n=8) or folate-deficient (n=12) version of an AIN-93G-based diet over the course of 18 days. Error bars indicate standard deviation of rat weights.

5.3.2 Results

The plasma formate concentration of animals fed either a folate-replete or folate-deficient AIN-93G-based diet supplemented with individual dietary formate precursors is shown in Figures 5.15 and 5.16 respectively. Among the folate-replete rats, only those given extra histidine showed a significantly increased plasma formate concentration. Among those rats given the folate-deficient diet, only supplementation with choline significantly increased plasma formate concentration; extra glycine significantly decreased plasma formate concentration.

No significant changes were noted in the urinary formate excretion of animals ingesting the folate-replete diet together with extra dietary formate precursors (Figure 5.17). Those folate-deficient animals given extra choline or tryptophan excreted significantly more formate in the urine than did the unsupplemented folate-deficient control (Figure 5.18).

Choline supplementation did not decrease plasma homocysteine compared to other supplementations/control in the folate-replete grouping (Figure 5.19). However, a significant decrease in plasma homocysteine was noted in folate deficient animals supplemented with extra choline(Figure 5.20). Choline was of specific interest in the context of plasma homocysteine because its metabolite betaine can be used by BHMT to create methionine from homocysteine, thereby lowering total plasma homocysteine levels. The other amino acids, lacking this ability, were grouped together for the purposes of this particular analysis.
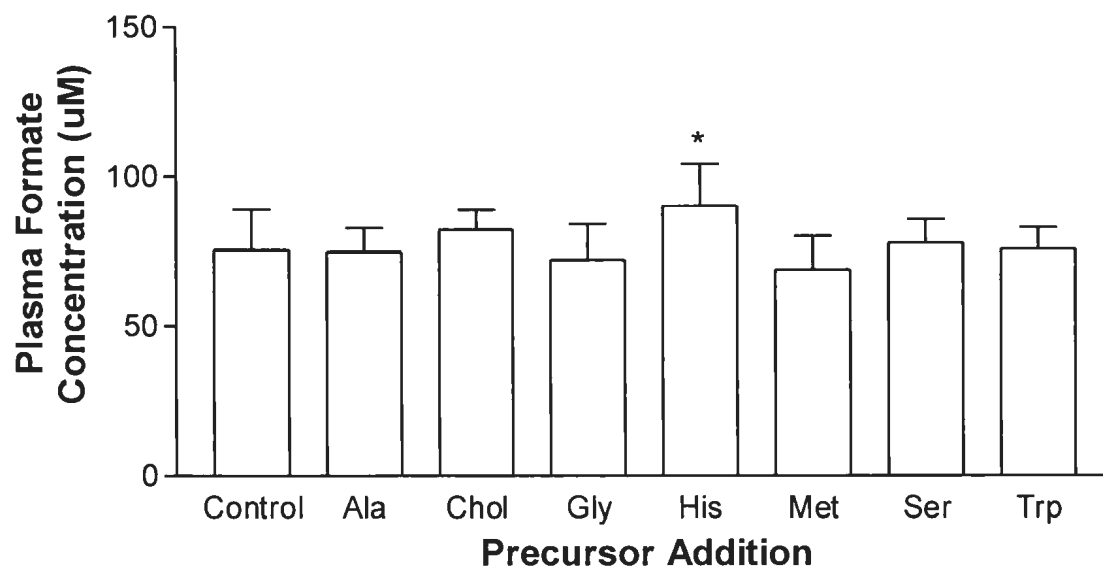
Figure 5.15. Plasma formate concentration for rats fed a folate-replete, AIN-93G-based diet for 18 days, supplemented with an extra 46 mmol/kg diet of individual one-carbon precursors for the final 5 days. Bars represent the mean of a group; error bars are standard deviation (n=8 control, n=4 supplemented groups). One asterisk indicates P≤0.05. Statistics were carried out by one-way ANOVA with comparisons of each experimental group against the combined unsupplemented control plus alanine groups.
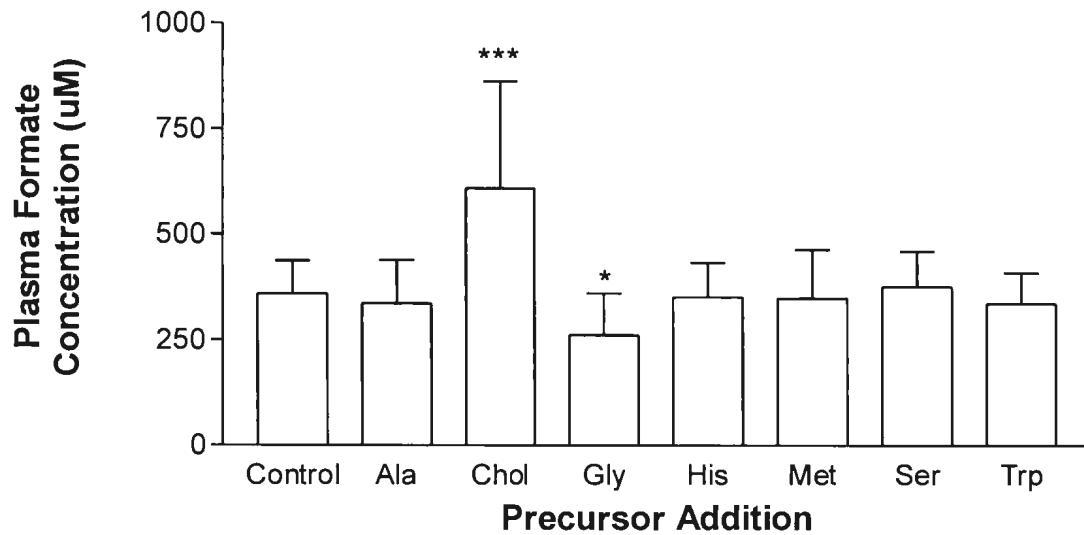
Figure 5.16. Plasma formate concentration for rats fed a folate-deficient, AIN-93G-based diet for 18 days, supplemented with an extra 46 mmol/kg diet of individual one-carbon precursors for the final 5 days. Bars represent the mean of a group; error bars are standard deviation (n=12 control, n=6 supplemented groups). One asterisk indicates P≤0.05, three asterisks indicates P≤0.001. Statistics were carried out by one-way ANOVA with comparisons of each experimental group against the combined unsupplemented control plus alanine groups.
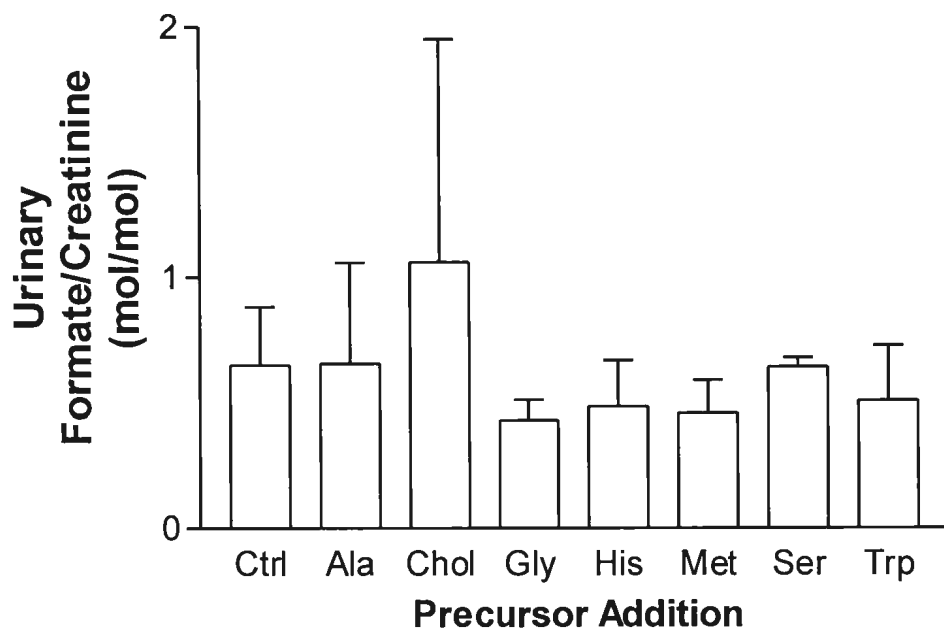
Figure 5.17. 24 hour formate excretion, normalized to creatinine excretion, in the urine of rats fed a folate-replete, AIN-93G-based diet for 18 days, supplemented with an extra 46 mmol/kg diet of individual one-carbon precursors for the final 5 days. Bars represent the mean of a group; error bars are standard deviation (n=8 control, n=3-4 supplemented groups). No significant differences were found. Statistics were carried out by one-way ANOVA with comparisons of each experimental group against the combined unsupplemented control plus alanine groups.
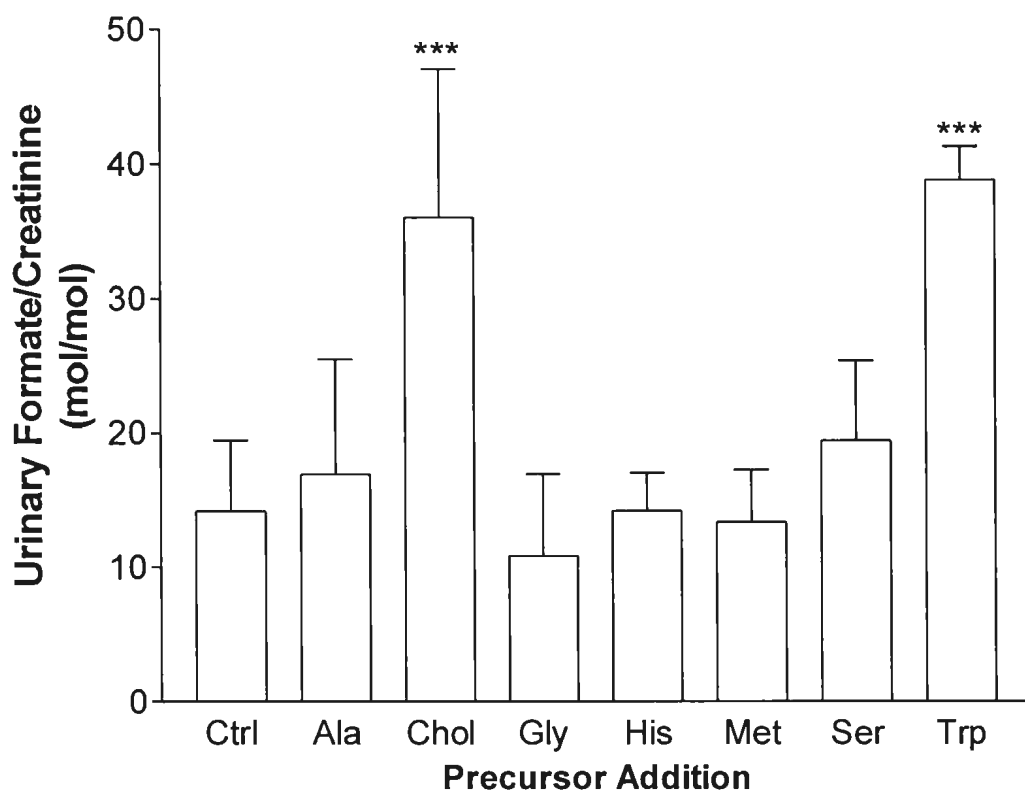
Figure 5.18. 24 hour formate excretion, normalized to creatinine excretion, in the urine of rats fed a folate-deficient, AIN-93G-based diet for 18 days, supplemented with an extra 46 mmol/kg diet of individual one-carbon precursors for the final 5 days. Bars represent the mean of a group; error bars are standard deviation (n=11 control, n=4-6 supplemented groups). Three asterisks indicate $P \leq 0.001$. Statistics were carried out by one-way ANOVA with comparisons of each experimental group against the combined unsupplemented control plus alanine groups.
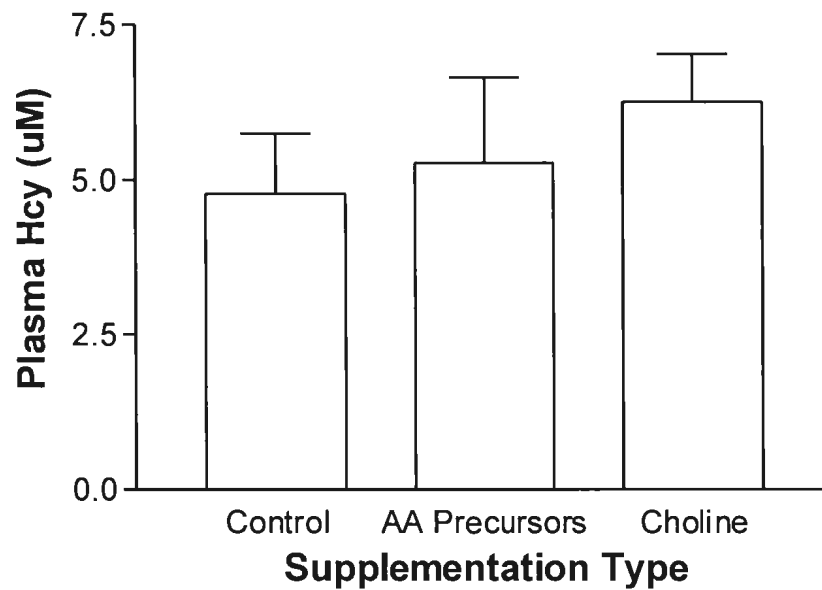
Figure 5.19. Plasma homocysteine concentration in rats fed a folate-replete, AIN-93G-based diet for 18 days (supplemented with an extra 46 mmol/kg diet of individual one-carbon precursors for the final 5 days). The AA precursors group consisted of all the supplemented animals except for those provided with extra choline. Bars indicate mean; error bars are standard deviation (n=5 control, n=14 AA precursors, n=4 choline). Statistics were carried out by one-way ANOVA with comparisons against the unsupplemented control.
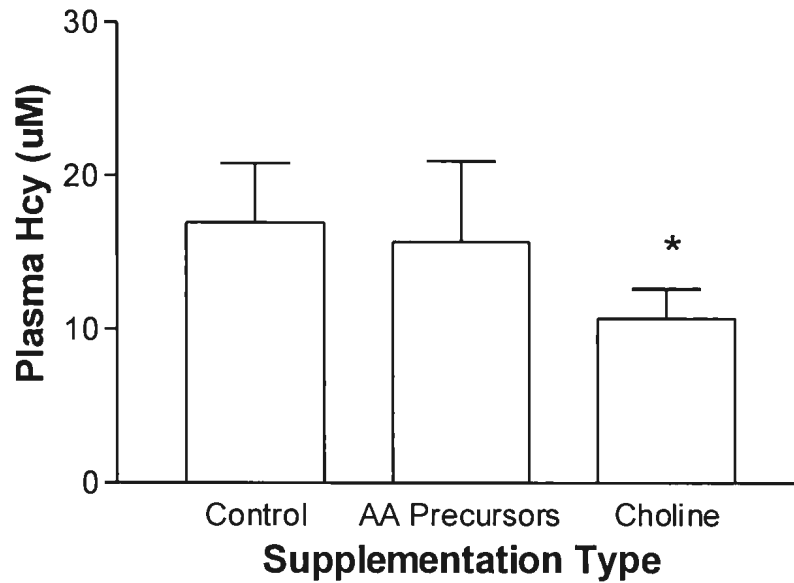
Figure 5.20. Plasma homocysteine concentration in rats fed a folate-deficient AIN 93G diet for 18 days (supplemented with an extra 46 mmol/kg diet of individual one-carbon precursors for the final 5 days). The AA precursors group consisted of all the supplemented animals except for those provided with extra choline. Bars indicate mean; error bars are standard deviation (n=7 control, n=17 AA precursors, n=6 choline). One asterisk indicates P≤0.05. Statistics were carried out by one-way ANOVA with comparisons against the unsupplemented control.

5.4 Comparison of 1C Precursor Supplementation Studies

We compared the baseline plasma formate concentrations between rats fed the folate-replete version of each diet, as well as between rats fed the folate-deficient version of each diet (Figure 5.21 (a) and (b) respectively). No significant difference exists on the basis of diet origin on the folate-replete level. However, rats fed the folate-deficient version of the Dyets diet (cat. #517777) had plasma formate levels significantly lower than rats fed the folate-deficient form of the AIN-93G-based diet.

The same trend exists when a similar comparison is made for urinary formate excretion (normalized to creatinine excretion). Figure 5.22 (a) compares urinary formate excretion between rats fed the folate-replete versions of each diet, while (b) compares urinary formate excretion between rats fed the folate-deficient version of either diet. No significant difference exists between the folate-replete versions. However, rats fed the Dyets (cat. #517777) folate-deficient diet excrete significantly lower quantities of formate compared to rats fed the folate-deficient version of the AIN-93G-based diet.

Since the folate-replete versions of each diet resulted in comparable plasma formate levels , we compared the folate-replete version of each diet supplemented with either histidine or serine with each other (5.23 (a) and (b) respectively). A comparison of the plasma formate levels, rather than urinary levels, was practical due to more consistent standard deviations in the plasma data (eg. unequal SDs – Figure 5.22 a). Histidine was of interest because it produced a plasma formate concentration significantly higher than the unsupplemented folate-replete control in both of the 1C precursor supplementation studies. Although serine only produced a significant

(a)

(b)
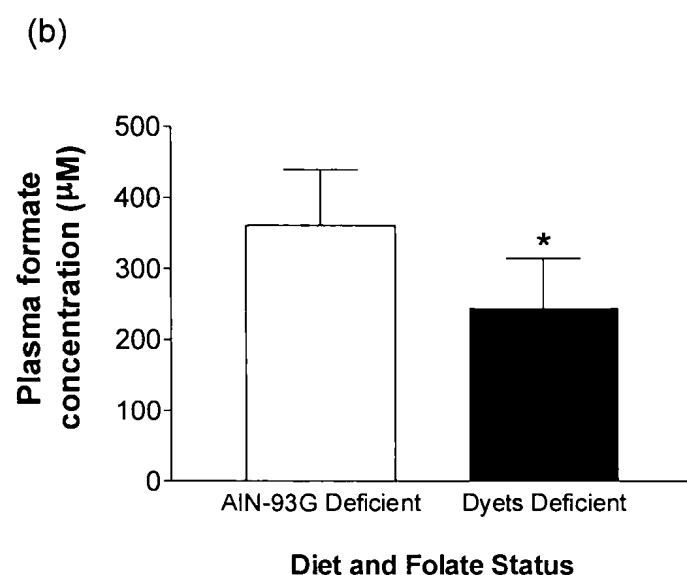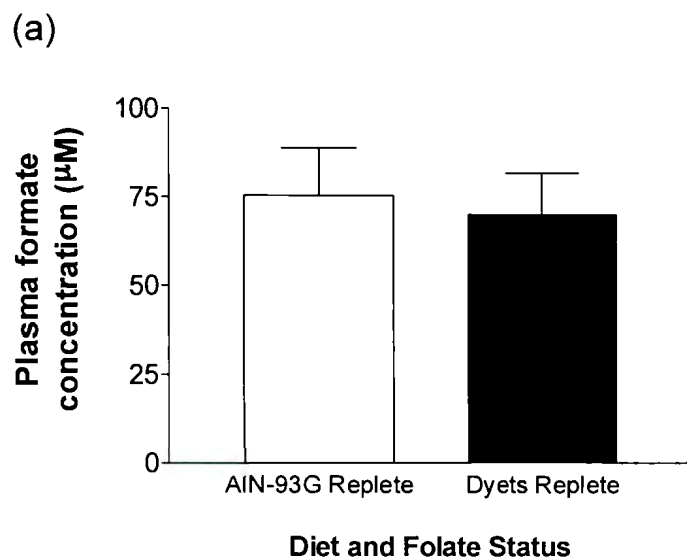
Figure 5.21. The plasma formate concentration of rats fed either an AIN-93G-based diet or a Dyets Inc diet (for 18 and 15 days respectively). (a) compares the folate-replete versions of these diets, and (b) compares the folate-deficient versions of these diets. One asterisk indicates a significance of $P<0.05$ by a two-tailed t-test.

(a)
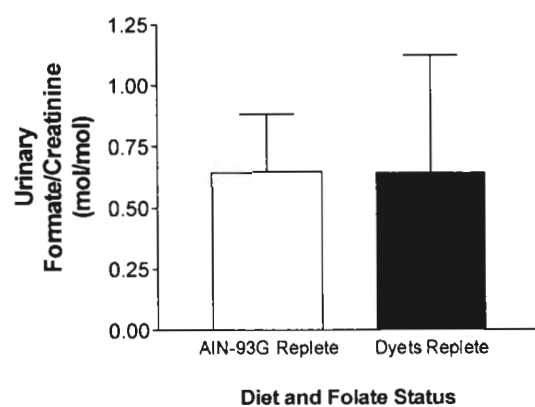
(b)
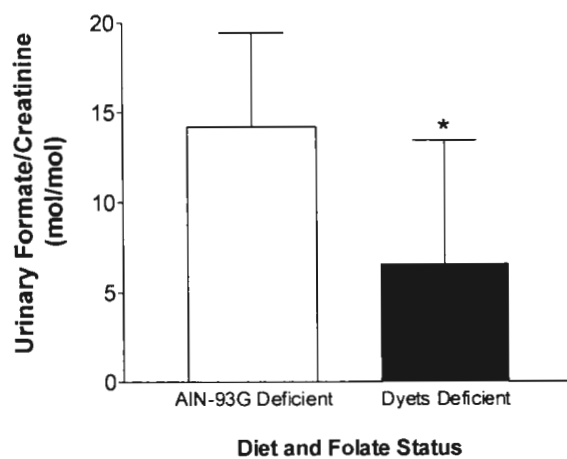
Figure 5.22. 24 hour formate excretion, normalized to creatinine excretion, of rats fed either an AIN-93G-based diet or a Dyets Inc diet (for 18 and 15 days respectively). (a) compares the folate-replete forms of these diets, and (b) compares the folate-deficient forms of these diets. One asterisk indicates a significance of P<0.05 by a two-tailed t-test.

(a)
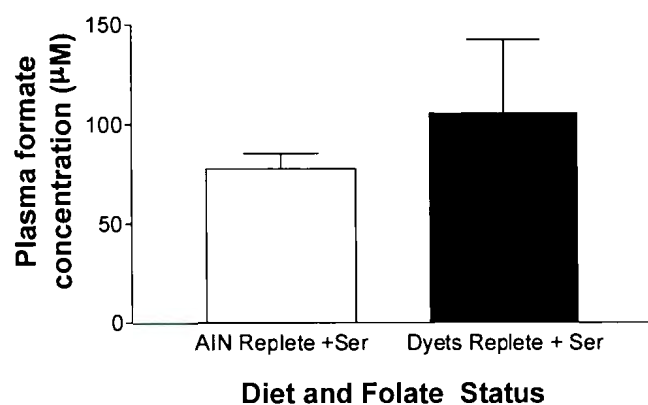
(b)
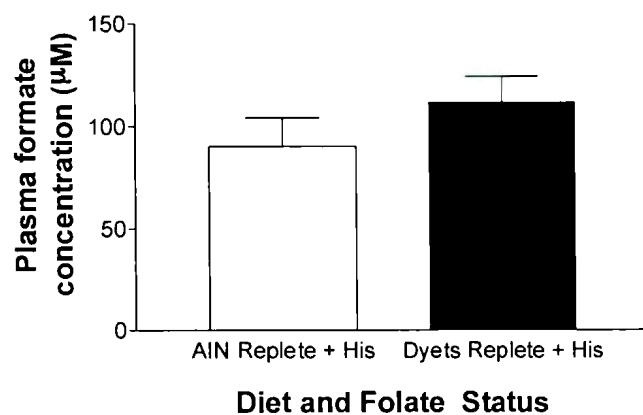
Figure 5.23. The plasma formate concentrations of rats fed either an AIN-93G-based diet or a Dyets Inc diet (for 18 and 15 days respectively). (a) compares the folate-replete forms of these diets supplemented with extra serine, and (b) compares the folate-replete forms of these diets supplemented with extra histidine. Details of the supplementations are provided in Appendices C and D for the AIN-93G-based diet and the Dyets diet respectively. No significant differences were found.

increase in the formate in the Dyets 1C precursor supplementation study, we noted

that the baseline AIN-93G has several fold more serine than the baseline Dyets diet, so

a comparison was deemed worthwhile in this case. Neither of these comparisons

(serine or histidine) was found to vary significantly on the basis of the diet.

5.5 Analysis

Our switch from the Dyets Inc. L-amino acid-defined diet to the AIN-93G-based

diet necessitated a repetition of the dietary one-carbon precursor supplementation

experiment. This gave us the opportunity to compare the results of these two

experiments.

We noted that plasma formate is significantly increased in both studies among

folate-replete, histidine-supplemented rats compared to the folate-replete controls.

Similarly, we note that in both experiments, the plasma formate concentration

decreased among folate-deficient, glycine supplemented rats compared to the folate-

deficient controls. This decrease in formate may be due to the fact that SHMT is a

reversible enzyme. An excess of glycine could be used to produce serine, drawing from

the one-carbon pool in the process.

Data from the initial 1C precursor supplementation study (using Dyets)

indicated that serine supplementation among folate-replete rats resulted in an increase

in plasma formate concentration over the folate-replete controls, an observation which

was mirrored by an increase in urinary formate excretion in this group. This was not

found in the AIN-93G-based study, a finding we could attribute to the fact that the AIN-

93G-based diet has 3 times the amount of serine as the base Dyets Inc. #517777 diet (as noted in the diet comparison featured in Appendix B).

Choline supplementation in the folate-deficient AIN-93G-based diet elevated the plasma formate concentration compared to the folate-deficient unsupplemented control. This is mirrored in the urinary formate excretion. This suggests that the choline catabolism pathway may be a significant source of free formate in these rats.

Although we note no increase in the plasma formate concentration as a result of tryptophan supplementation in rats fed a folate-deficient AIN-93G-based diet (Figure 5.18), we do see an increase in urinary formate excretion. This may be due to the fact that tryptophan has been shown to increase the glomerular filtration rate(57) which may increase the urinary loss of formate. However this does not explain why a similar increase informate excretion is missing in folate-replete rats.

Since we found no difference in hepatic catalase activity between the folate-replete and folate-deficient rats, we cannot attribute changes in the formate levels to catalase. However, it is important to note that this was an in vitro assay of activity, and thus not necessarily representative of the activities we would see in a whole rat.

Chapter Six – General Conclusions and Future Work

6.1 General Conclusions and Future Work

The work presented in this thesis will serve to increase the understanding of formate in the context of one-carbon metabolism. The baseline plasma formate concentration, urinary formate excretion and the underlying rate of formate production were all shown to change significantly during folate-deficiency. Formate could therefore be used as a marker for impaired folate metabolism. With further study, it is conceivable that formate could be used as a general marker of impaired one-carbon metabolism (such as deficiencies in the other B vitamins involved in 1C metabolism such as B6, B12 or riboflavin, or inborn errors in the various relevant enzymes).

The optimization of the coupled FDH/diaphorase assay was instrumental in the work presented in this thesis. A key requirement of any endpoint assay is that, after the component reactions have come to completion, the end result should not change with time. The persistent rise in absorbance (the "creep") seen in alternate versions of this assay meant that it was impossible to determine an absolute formate concentration. The use of the PD-10 desalting column for FDH purification paired with the INT/diaphorase dye-reduction system resulted in a clean plateau, and a plasma formate concentration that could be reported with confidence. This has resulted in a robust, economical assay that will allow for the determination of plasma formate concentrations in virtually any laboratory setting. The optimizations we have made do not require excessive additional resources or time to implement. Additionally, it can be adapted to a microplate format as well as a traditional spectrophotometric setup, depending on equipment availability. Given that formate metabolism is integral to 1C

metabolism in general, plasma formate determination will be useful in many areas of this field of research.

The sodium ^{13}C-formate constant infusion study indicated that formate production is a significant fate for some or all of the 1C precursors found in the diet. 35% of the 1C precursors ingested in one day gave rise to endogenous formate production in folate-replete rats. Moderate folate-deficiency resulted in only 20% of the ingested potential dietary 1C precursors leading to free formate. After accounting for amino acids destined for net protein synthesis, we found that 44% and 24% of resulting potential 1C precursors were used to produce formate in folate-replete and folate-deficient rats respectively. It remains to be seen whether particular precursors out of this group of amino acids or choline bear a greater burden in 1C production, because our infusion experiment was unable to differentiate between formate produced from the various folate-associated pathways. The fact that 44% of 1C precursors are destined to become formate indicates that 1C metabolism is a significant fate for the 5 amino acids studied (and choline).

On the basis of our two dietary 1C supplementation experiments, we suggest that 1C production may be a significant fate of choline, histidine and serine. More elaborate studies would be necessary to verify this, and subsequently make quantifiable statements about the relative importance of particular precursors for creating and maintaining the formate pool. Future tracer experiments could use labelled-1C precursors of interest to determine which precursors successfully transfer significant quantities of ^{13}C into the formate pool. This would confirm or refute the

importance of each 1C precursor to the health of the 1C pool. This could be taken a step further by seeing which potential 1C precursors successfully transfer ^{13}C label to newly synthesized thymidylate and purine synthesis or into the trans-methylation cycle.

Gaining a more profound and in depth understanding of formate metabolism has value beyond a purely fundamental scientific understanding of the metabolic pathways involved. In addition to the involvement of folate described in this thesis, formate metabolism is dependent on the presence of several other B vitamins such as riboflavin and B12. Accordingly, there is the potential for formate to act as a biomarker for both vitamin deficiencies and impairments in the relevant pathways. The link between folate and the provisioning of DNA bases to rapidly dividing cells (such as in the development of embryos, or in tumors) has long been a topic of interest. Given the close relationship that we have demonstrated not only between folate and formate levels, but also between folate levels and the rate of endogenous formate production, formate must be considered as an important element in the arena of one-carbon metabolism. Further research will help to elucidate the relationship between this apparently important pool of free one-carbon units, their incorporation into the folate-associated one-carbon pool, and the demands on this resource from the body's various one-carbon requiring pathways.

Bibliography

1. Scott, J. M., and Weir, D. G. (1998) Folic acid, homocysteine and one-carbon metabolism: a review of the essential biochemistry, *J Cardiovasc Risk 5*, 223-227.

2. Cook, R. J. (2001) Folate Metabolism, In *Homocysteine in Health and Disease* (Carmel, R., and Jacobsen, D., Eds.), Cambridge University Press.

3. Bree, A. d., Dusseldorp, M. v., Brouwer, I. A., Hof, K. H. v. h., and Steegers-Theunissen, R. P. M. (1997) Folate intake in Europe: recommended, actual and desired intake, *Eur J Clin Nutr 51*, 643-660.

4. Appling, D. (1991) Compartmentation of folate-mediated one-carbon metabolism in eukaryotes, *FASEB 5*, 2645-2651.

5. Melse-Boonstra, A., de Bree, A., Verhoef, P., Bjørke-Monsen, A. L., and Verschuren, W. M. M. (2002) Dietary Monoglutamate and Polyglutamate Folate Are Associated with Plasma Folate Concentrations in Dutch Men and Women Aged 20–65 Years, *J Nutr 132*, 1307-1312.

6. McNulty, H., and Pentieva, K. (2004) Folate bioavailability, *Proc Nutr Soc 63*, 529-536.

7. Naughton, C. A., Chandler, C. J., Duplantier, R. B., and Halsted, C. H. (1989) Folate absorption in alcoholic pigs: in vitro hydrolysis and transport at the intestinal brush border membrane, *Am J Clin Nutr 50*, 1436-1441.

8. Tibbetts, A. S., and Appling, D. R. (2010) Compartmentalization of Mammalian Folate-Mediated One-Carbon Metabolism, *Annu Rev Nutr 30*, 57-81.

9. Bailey, S. W., and Ayling, J. E. (2009) The extremely slow and variable activity of dihydrofolate reductase in human liver and its implications for high folic acid intake, *PNAS 106*, 15424-15429.

10. Springs, B., and Haake, P. (1977) Equilibrium constants for association of guanidinium and ammonium ions with oxyanions: The effect of changing basicity of the oxyanion, *Bioorg Chem 6*, 181-190.

11. Weinhouse, S., and Friedmann, B. (1954) A study of formate production in normal and folic acid-deficient rats, *J Biol Chem 210*, 423-433.

12. Lamarre, S. G., Molloy, A. M., Reinke, S. N., Sykes, B. D., Brosnan, M. E., and Brosnan, J. T. (2011) Formate can differentiate between hyperhomocysteinemia due to impaired remethylation and impaired transsulfuration, *Am J Physiol Endocrinol Metab*.

13.	Anderson, D. D., Eom, J. Y., and Stover, P. J. (2012) Competition between Sumoylation and Ubiquitination of Serine Hydroxymethyltransferase 1 Determines Its Nuclear Localization and Its Accumulation in the Nucleus, *J Biol Chem 287*, 4790-4799.

14.	Stover, P. J., Chen, L. H., Suh, J. R., Stover, D. M., Keyomarsi, K., and Shane, B. (1997) Molecular Cloning, Characterization, and Regulation of the Human Mitochondrial Serine Hydroxymethyltransferase Gene, *J Biol Chem 272*, 1842-1848.

15.	Davis, S. R., Stacpoole, P. W., Williamson, J., Kick, L. S., Quinlivan, E. P., Coats, B. S., Shane, B., Bailey, L. B., and Gregory, J. F. (2004) Tracer-derived total and folate-dependent homocysteine remethylation and synthesis rates in humans indicate that serine is the main one-carbon donor, *Am J Physiol Endocrinol Metab 286*, E272-E279.

16.	Beaudin, A. E., Abarinov, E. V., Noden, D. M., Perry, C. A., Chu, S., Stabler, S. P., Allen, R. H., and Stover, P. J. (2011) Shmt1 and de novo thymidylate biosynthesis underlie folate-responsive neural tube defects in mice, *Am J Clin Nutr 93*, 789-798.

17.	Anderson, D. D., and Stover, P. J. (2009) SHMT1 and SHMT2 Are Functionally Redundant in Nuclear De novo Thymidylate Biosynthesis, *PLoS 1 4*, e5839.

18.	Narisawa, A., Komatsuzaki, S., Kikuchi, A., Niihori, T., Aoki, Y., Fujiwara, K., Tanemura, M., Hata, A., Suzuki, Y., Relton, C. L., Grinham, J., Leung, K.-Y., Partridge, D., Robinson, A., Stone, V., Gustavsson, P., Stanier, P., Copp, A. J., Greene, N. D. E., Tominaga, T., Matsubara, Y., and Kure, S. (2012) Mutations in genes encoding the glycine cleavage system predispose to neural tube defects in mice and humans, *Hum Mol Gen 21*, 1496-1503.

19.	Brosnan, J. T., and Brosnan, M. E. (2006) The Sulfur-Containing Amino Acids: An Overview, *J Nutr 136*, 1636S-1640S.

20.	Cook, R. J., and Wagner, C. (1984) Glycine N-methyltransferase is a folate binding protein of rat liver cytosol, *PNAS 81*, 3631-3634.

21.	Finkelstein, J. D., Martin, J. J., and Harris, B. J. (1988) Methionine metabolism in mammals. The methionine-sparing effect of cystine, *J Biol Chem 263*, 11750-11754.

22.	Krebs, H. A., and Hems, R. (1976) The regulation of the degradation of methionine and of the one-carbon units derived from histidine, serine and glycine, *Adv Enzyme Regul 14*, 493-513.

23. Slow, S., and Garrow, T. A. (2006) Liver Choline Dehydrogenase and Kidney Betaine-Homocysteine Methyltransferase Expression Are Not Affected by Methionine or Choline Intake in Growing Rats, *J Nutr 136*, 2279-2283.

24. Porter, D. H., Cook, R. J., and Wagner, C. (1985) Enzymatic properties of dimethylglycine dehydrogenase and sarcosine dehydrogenase from rat-liver, *Arch Biochem Biophys 243*, 396-407.

25. Hum, D. W., Bell, A. W., Rozen, R., and MacKenzie, R. E. (1988) Primary structure of a human trifunctional enzyme. Isolation of a cDNA encoding methylenetetrahydrofolate dehydrogenase-methenyltetrahydrofolate cyclohydrolase-formyltetrahydrofolate synthetase, *J Biol Chem 263*, 15946-15950.

26. Gál, E. M., and Sherman, A. D. (1980) l-Kynurenine Its synthesis and possible regulatory function in brain, *Neurochem Res 5*, 223-239.

27. Zubay, G. (1983) *Biochemistry*, Addison Wesley.

28. Fukushima, H., Grinstead, G. F., and Gaylor, J. L. (1981) Total enzymic synthesis of cholesterol from lanosterol. Cytochrome b5-dependence of 4-methyl sterol oxidase, *J Biol Chem 256*, 4822-4826.

29. Mihalik, S. J., Rainville, A. M., and Watkins, P. A. (1995) Phytanic Acid α-oxidation in Rat Liver Peroxisomes, *Eur J Biochem 232*, 545-551.

30. Ekins, B. R., Rollins, D. E., Duffy, D. P., and Gregory, M. C. (1985) Standardized Treatment of Severe Methanol Poisoning With Ethanol and Hemodialysis, *West J Med 142*, 337-340.

31. Pike, S. T., Rajendra, R., Artzt, K., and Appling, D. R. (2010) Mitochondrial C1-Tetrahydrofolate Synthase (MTHFD1L) Supports the Flow of Mitochondrial One-carbon Units into the Methyl Cycle in Embryos, *J Biol Chem 285*, 4612-4620.

32. Barlowe, C. K., and Appling, D. R. (1988) In-vitro evidence for the involvement of mitochondrial folate metabolism in the supply of cytoplasmic one-carbon units, *Biofactors 1*, 171-176.

33. Ho, V., Massey, T. E., and King, W. D. (2011) Thymidylate synthase gene polymorphisms and markers of DNA methylation capacity, *Mol Gen Metab 102*, 481-487.

34. Aebi, H. (1984) [13] Catalase in vitro, In *Methods Enzymol* (Lester, P., Ed.), pp 121-126, Academic Press.

35. Drysdale, G. R., Plaut, G. W. E., and Lardy, H. A. (1951) The relationship of folic acid to formate metabolism in the rat - formate incorporation into purines, *J Biol Chem 193*, 533-538.

36. Weinhouse, S., and Friedmann, B. (1952) Study of precursors of formate in the intact rat, *J Biol Chem 197*, 733-740.

37. Plaut, G. W. E., Betheil, J. J., and Lardy, H. A. (1950) The relationship of folic acid to formate metabolism in the rat, *J Biol Chem 184*, 795-805.

38. Shive, W., Ackermann, W. W., Gordon, M., Getzendaner, M. E., and Eakin, R. E. (1947) 5(4)-amino-4(5)-imidazolecarboxamide, a precursor of purines, *J Am Chem Soc 69*, 725-726.

39. Bills, N., Koury, M., Clifford, A., and Dessypris, E. (1992) Ineffective hematopoiesis in folate-deficient mice, *Blood 79*, 2273-2280.

40. Walzem, R. L., and Clifford, A. J. (1988) Folate Deficiency in Rats Fed Diets Containing Free Amino Acids or Intact Proteins, *J Nutr 118*, 1089-1096.

41. Reeves, P. G., Nielsen, F. H., and G.C. Fahey, J. (1993) AIN-93 Purified Diets for Laboratory Rodents: Final Report of the American Institute of Nutrition Ad Hoc Writing Committee on the Reformulation of the AIN-76A Rodent Diet, *J Nutr 123*, 1939-1951.

42. Horne, D. W., and Patterson, D. (1988) Lactobacillus casei microbiological assay of folic acid derivatives in 96-well microtiter plates, *Clin Chem 34*, 2357-2359.

43. Saude, E., and Sykes, B. (2007) Urine stability for metabolomic studies: effects of preparation and storage, *Metabolomics 3*, 19-27.

44. Grady, S., and Osterloh, J. (1986) Improved Enzymic Assay for Serum Formate with Colorimetric Endpoint, *J Anal Toxicol 10*, 1-5.

45. Kage, S., Kudo, K., Ikeda, H., and Ikeda, N. (2004) Simultaneous determination of formate and acetate in whole blood and urine from humans using gas chromatography–mass spectrometry, *J Chromatogr*, 113-117.

46. Yuen, P. S. T., Dunn, S. R., Miyaji, T., Yasuda, H., Sharma, K., and Star, R. A. (2004) A simplified method for HPLC determination of creatinine in mouse serum, *Am J Physiol Renal Physiol 286*, F1116-F1119.

47. Wyss, M., and Kaddurah-Daouk, R. (2000) Creatine and Creatinine Metabolism, *Physiol Rev 80*, 1107-1213.

48. Jackson, S. (1966) Creatinine in Urine as an Index of Urinary Excretion Rate, *Health Phys 12*, 843-850.

49. Vester, B., and Rasmussen, K. (1991) High Performance Liquid Chromatography Method for Rapid and Accurate Determination of Homocysteine in Plasma and Serum, *Eur J Clin Chem Clin Biochem 29*, 549-554.

50. Avilova, T. V., Egorova, O. A., Ioanesyan, L. S., and Egorov, A. M. (1985) Biosynthesis, isolation and properties of NAD-dependent formate dehydrogenase from the yeast Candida methylica, *Eur J Biochem 152*, 657-662.

51. Ishiyama, M., Miyazono, Y., Sasamoto, K., Ohkura, Y., and Ueno, K. (1997) A highly water-soluble disulfonated tetrazolium salt as a chromogenic indicator for NADH as well as cell viability, *Talanta 44*, 1299-1305.

52. Wolfe, R. R., and Chinkes, D. L. (2004) *Isotope tracers in metabolic research: principles and practice of kinetic analysis*, 2e ed., Wiley-Liss.

53. Annison, E. F., and White, R. R. (1962) Formate Metabolism in Sheep, *Biochem J 84*, 552-557.

54. Ferrell, C. L., and Koong, K. J. (1986) Influence of Plane of Nutrition on Body Composition, Organ Size and Energy Utilization in Sprague Dawley Rats, *J Nutr 116*, 2525-2535.

55. Rafecas, I. (1994) Whole-rat protein content estimation: applicability of the N x 6.25 factor, *Brit J Nutr 72*, 199-209.

56. Kapur, B. M., Vandenbroucke, A. C., Adamchik, Y., Lehotay, D. C., and Carlen, P. L. (2007) Formic Acid, a Novel Metabolite of Chronic Ethanol Abuse, Causes Neurotoxicity, Which Is Prevented by Folic Acid, *Alcoholism: Clinical and Experimental Research 31*, 2114-2120.

57. Martinsons, A., Rudzite, V., Cernevskis, H., Mihailova, I., and Smeltere, Z. (2003) The influence of L-tryptophan peroral load on glomerular filtration rate in chronic glomerulonephritis and chronic renal failure, In *Developments in Tryptophan and Serotonin Metabolism* (Allegri, G. C. C. V. L. R. E. S. H. V. L., Ed.), pp 337-345.

Appendices
Appendix A – Plasma formate under a variety of physiological situations.

Samples from our laboratory, covering a range of common physiological conditions in the rat, were assayed to determine the plasma formate concentration using the coupled enzymatic assay described in section 2.6.1. These are provided in Table A1.

The low and high protein diets were based on an AIN-93G formula, but with 0, 20 or 50% casein by mass, respectively. The difference from the normal 20% casein was offset proportionally by all carbohydrate sources. The rats were fed for a week on this diet.

Artificial diabetes was induced in rats using streptozotocin (100 mg/kg body weight,in saline) to destroy the pancreatic β-cells responsible for insulin production. Diabetic controls were monitored, and given sufficient insulin to maintain the glucose concentration inside the normal physiological range. This protocol was continued for several days prior to sampling of blood.

Neonatal pups were removed from their litters and blood was sampled, while weanling rats were obtained at ~70 g, and blood sampled.

Fed rats were obtained at 200 g, and fed a chow diet ad libitum for 48 hours and blood was sampled. Fasted rats were obtained at 200 g, and received no food for 48 hours prior to blood being sampled. In both cases, animals had free access to water.

Table A1. Plasma formate in the rat in a number of physiological conditions. Concentrations were determined by coupled enzyme assay (*formate dehydrogenase/ diaphorase*). Plasma formate concentration is given as the concentration (μM), with the standard deviation in parenthesis.

Physiological Condition	Plasma formate concentration (μM)	Sample size
Low Protein (0%)	69 (20)	5
Normal Protein (20%)	77 (11)	5
High Protein (50%)	55 (11)	5
Diabetic Control	60 (7)	3
Diabetic	67 (16)	5
Neonatal pups	150 (17)	4
Weanling (70 g)	173 (75)	3
Fed	34 (4)	4
Fasted	38 (5)	4

Note: With the exception of the fed and fasted rats, all animal care work presented in this table was carried out by Drs. Simon Lamarre and Robin Da Silva. The assaying of plasma for all samples was carried out by the author of this thesis and Mr. Luke Macmillan.

Appendix B – Comparison of amino acid composition of diets

Table B1. A comparison of the quantities of amino acids present in two experimental diets that can be used to induce folate-deficiency in rats. The central column indicates the fold difference for each amino acid. A red bar indicates that a greater quantity is present in the Dyets Inc. (FD - #517777, FR - #517802) amino acid-defined diet, and is the composition reported form Dyets Inc.. A blue bar indicates that there is a greater quantity in the AIN-93G -based diet (casein-based), and is the typical casein amino acid profile, as reported in the AIN-93 Diet Report.

Dyets Inc. (cat #517777)		Fold Difference	AIN-93G	
Amino Acid	g AA /kg diet		Amino Acid	g AA/ kg Diet
Arg	11.2	-1.8	Arg	6.4
His	3.3	1.4	His	4.6
Asn	6.82		Asn	--
Lys	18	-1.4	Lys	13
Tyr	3.5	2.7	Tyr	9.3
Trp	1.74	1.2	Trp	2.1
Phe	11.6	-1.3	Phe	8.8
Met	8.2	-1.8	Met	4.6
Cys	3.5	1.1	Cys	3.7
Thr	8.2	-1.2	Thr	6.7
Leu	11.1	1.4	Leu	15.4
Ile	8.2	1.0	Ile	8.5
Val	8.2	1.2	Val	10
Gly	23.3	-7.3	Gly	3.2
Pro	3.5	5.9	Pro	20.5
Glu	35	1.0	Glu	36.3
Ala	3.5	1.3	Ala	4.6
Asp	3.5	3.5	Asp	12.2
Ser	3.5	2.8	Ser	9.7
Gln	--		Gln	--

Appendix C – Experimental diets (compositions, mineral mixes, and vitamin mixes)

Table C1. List of ingredients for Dyets Inc. folate deficient L-amino acid-defined diet (Cat. #517777). The full amino acid profile is found in Appendix B.

Ingredient	g/kg
Total L-amino acids	176
Dextrin	397
Cellulose (microcrystalline)	50
Sucrose	197
Sodium acetate	8
Corn oil (g)	100
Choline chloride	2
Succinyl sulfathiazole	10
Mineral mix #210020	50
Vitamin mix #317759 (folic acid free)	10

Table C2. List of ingredients for production of AIN-93G-based diet

Ingredient	g/kg diet
Cornstarch	387.5
High-nitrogen casein	200
Dextrinized cornstarch	132
Sucrose	100
Soybean oil (g)	70
Fiber	50
Mineral mix (AIN-93G-MX)	35
Vitamin mix (AIN-93-VX)	10
Succinyl sulfathiazole	10
L-Cystine	3
Choline bitartrate	2.5
Tert-butylhydroquinone	0.014

Table C3. Mineral mix #210020 - Elements provided to 1 kg Dyets diet from 50g of mineral mix

Ingredient	g/kg
Calcium carbonate	14.6
Calcium phosphate, dibasic	0.17
Sodium chloride	12.4
Potassium phosphate, dibasic	17.2
Magnesium sulfate, anhydrous	2.45
Manganese sulfate, monohydrate	0.18
Ferric citrate, U.S.P.	0.63
Zinc carbonate, basic	0.058
Cupric carbonate, basic	0.054
Potassium iodide (mg)	0.250
Sodium selenite(mg)	0.495
Molybdic acid, ammonium salt (mg)	1.25
Chromium potassium sulfate, dodecahydrate (mg)	19
Sodium fluoride (mg)	2.5
Sucrose, finely powdered	2.09

Table C4. Vitamin mix #317759 - Vitamins provided to 1 kg Dyets diet from 10g of vitamin mix

Ingredient	mg/kg
Thiamin HCl	6
Riboflavin	6
Pyridoxine HCl	7
Nicotinic acid	0.3
Calcium pantothenate	16
Folic Acid	0
Biotin	0.2
Vitamin B12 (0.1%)	50
Vitamin A palmitate (500,000 IU/g)	8
Vitamin D3 (400,000 IU/g)	2.5
Vitamin E acetate (500 IU/g)	100
Menadione sodium bisulfite	50

A corresponding folate-replete diet was used for control purposes (Dyets Inc. Cat. # 517802), containing an identical vitamin mix supplemented by folic acid at a strength of 2 mg per kg complete diet. The balance of the 10g is made up of sucrose.

Table C5. Mineral mix (AIN-93G-MX) - Elements provided to 1 kg Dyets diet from 35g of mineral mix

Ingredient	mg/kg diet	Ingredient	mg/kg diet
Calcium	5000	Chromium	1
Phosphate	1561	Iodine	0.2
Potassium	3600	Selenium	0.15
Sodium	1019	Fluorine	1
Chloride	1571	Boron	0.5
Sulfur	300	Molybdenum	0.15
Magnesium	507	Silicon	5
Iron	35	Nickel	0.5
Copper	6	Lithium	0.1
Manganese	10	Vanadium	0.1
Zinc	30		

Table C6. Vitamin mix (AIN-93-VX) - Vitamins provided to 1 kg Dyets diet from 10g of vitamin mix

Ingredient	Unit/kg diet	Quantity
Thiamin HCl	mg	6
Riboflavin	mg	6
Pyridoxine HCl	mg	7
Niacin	mg	30
Calcium Pantothenate	mg	16
Folic Acid	mg	2
Biotin	mg	0.2
Cyanocobalamin (B12, 0.1%)	mg	25
Vitamin A Palmitate	IU	4000
Vitamin E Acetate	IU	75
Vitamin D3	IU	1000
Vitamin K1	mg	0.75

A corresponding folate-deficient AIN-93G-based diet was produced containing a similar vitamin mix, but lacking folic acid.
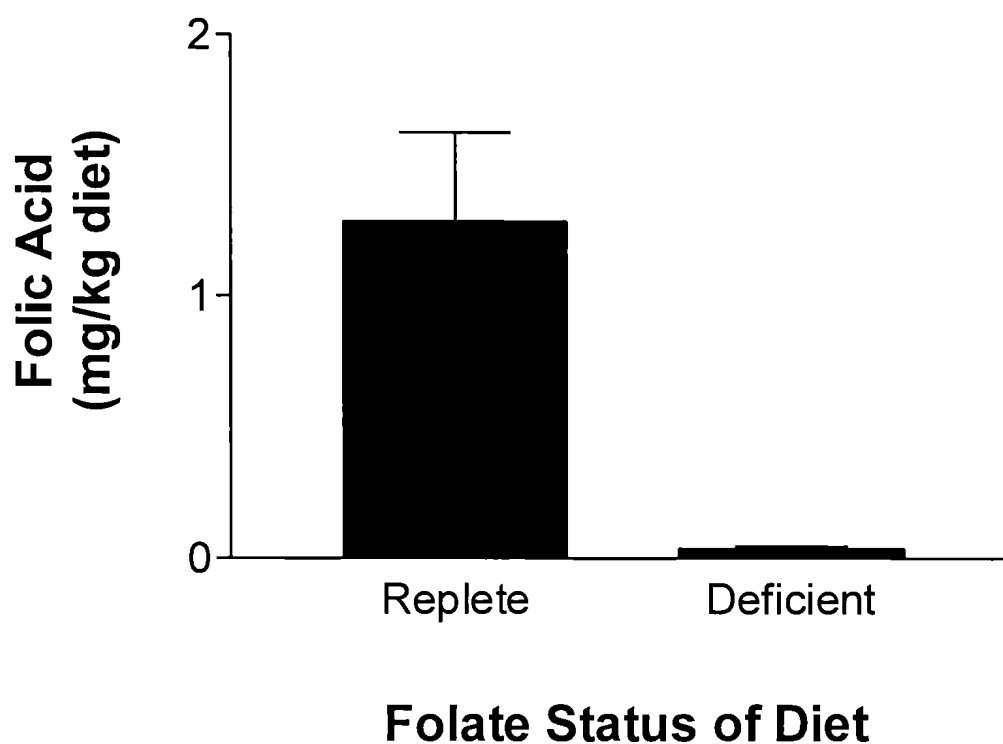
Folate Status of Diet

Figure C1. Folic acid content of the folate-replete (cat. #517802) and folate-deficient (cat. #517777) versions of the Dyets Inc. diet which are advertised as containing 2 mg and 0 mg of folic acid per kg of diet respectively. The values are given are the mean; error bars are standard deviation (n=6 for folate-replete, n=9 for folate-deficient). These measurements were performed by Dr. MacFarlane of Health Canada, based on a microbiological assay using L. Casei (42). Although the folate-replete diet yielded less folate than expected (~1.3 mg/kg diet instead of 2 mg/kg diet), the folate-deficient diet was almost completely free of folate contamination as required.

Appendix D – Dyets Inc. amino acid-defined diet (cat. #517777, #517802) 1C precursor supplementation trial diet modifications

Table D1. Molar quantity of 1C precursor added to 1kg of supplemented diet

Amino Acid	Molar quantity of 1C precursor added to 1 kg diet (mmol)	Molar quantity of L-alanine added to 1kg diet (mmol)
Glycine	310	0
L-Histidine	21	289
L-Tryptophan	9	301
L-Methionine	55	255
L-Alanine	310	0
L-Serine	33	277
Sarcosine	55	255
Dimethylglycine	55	255
Choline chloride	55	255

Table D2. Masses of 1C precursor and alanine added to 1kg of supplemented diet

Amino Acid	Mass of 1C precursor added to 1 kg diet(g)	Mass of L-alanine added to 1kg diet (g)
Glycine	23.25	0
L-Histidine	3.31	25.69
L-Tryptophan	1.71	26.78
L-Methionine	8.19	22.69
L-Alanine	27.59	0
L-Serine	3.5	24.63
Sarcosine	4.91	22.69
Dimethylglycine	5.56	22.69
Choline chloride	7.65	22.69

Dyets Inc. ships the amino acid-defined diet pre-mixed, so it is not possible to offset the 1C precursor and alanine supplementation by reducing other specific ingredients. When adding supplementations to these diets, the particular precursor and alanine were added to enough premixed diet to make up one kilogram. This meant that in the supplemented diets, all ingredients (from Table B1) were actually present in slightly lower quantities than the control (unsupplemented) diets. Since the combined masses of the supplemented 1C precursor/alanine never exceeded 10g (into ~990g of premixed diet), there was a ~1% variance between control and supplemented diets for the other ingredients.

Appendix E – AIN-93G-based 1C precursor supplementation trial diet modifications

Table E1. Quantity of 1C precursor added to 1kg of supplemented diet

1C Precursor	Molar quantity of 1C precursor added to 1 kg diet (mmol)	Molar Mass	Mass of 1C precursor added to 1 kg diet(g)
Serine	46	105	4.8
Tryptophan	46	204	9.4
Glycine	46	75	3.5
Alanine	46	89	4.1
Choline bitartrate	46	253	11.6
Histidine	46	155	7.1
Methionine	46	149	6.9

The AIN-93G-based diets are mixed in-house, allowing for the increase or decrease of specific ingredients as necessary. Accordingly, when supplementing the special experimental diets (as per the final column of Table D1), the quantity of corn starch was reduced correspondingly. As a result, with the exception of corn starch and the supplemented 1C precursor in question, the quantities of individual ingredients did not vary between the control diets and the supplemented diets.